First European Physical Society Conference on Gravitation
"Sapienza" Rome University
19-21 February, 2019

A new measurement of the Earth's gravitomagnetic field a century after the formulation of the Lense-Thirring effect

David M. Lucchesi (1,2,3), Luciano Anselmo (2), Massimo Bassan (3,4), Carmelo Magnafico (1,3), Carmen Pardini (2), Roberto Peron (1,3), Giuseppe Pucacco (3,4) and Massimo Visco (1,3)

david.lucchesi@inaf.it

1. Istituto di Astrofisica e Planetologia Spaziali (IAPS/INAF), Via Fosso del Cavaliere n. 100, 00133 Tor Vergata – Roma, Italy
2. Istituto di Scienza e Tecnologie della Informazione (ISTI/CNR), Via Moruzzi n. 1, 56124 Pisa, Italy
3. Istituto Nazionale di Fisica Nucleare (INFN), sezione di Roma Tor Vergata, Via della Ricerca Scientifica n. 1, 00133 Tor Vergata – Roma, Italy
4. Dipartimento di Fisica, Università di Tor Vergata, Via della Ricerca Scientifica n. 1, 00133 Tor Vergata – Roma, Italy

National Scientific Committee 2 (CSN2):
astroparticle physics experiments
www.infn.it

http://larase.roma2.infn.it

Summary

- The Lense-Thirring effect and gravitomagnetism
- The LARASE experiment and its goals
- The LASSOS model for the spin
- Thermal effects and their modelling
- Model for the Earth's gravitational field
- Precise orbit determination
- A new measurement of the Lense-Thirring effect
- Conclusions and future work

The Lense-Thirring effect and gravitomagnetism

Gravitomagnetism is a peculiarity of Einstein's theory of General Relativity

- it is strongly connected to the concepts of inertia (how it originates) and rotation (apparent forces like gravitational forces)
- ''inertia here arises from mass-energy there'', represents a link to Mach's ideas…
- Gravitomagnetism has no classical (Newtonian) gravitational counterpart, but it has a strong analogy with magnetism

Gravitoelectromagnetic fields $(\vec{E}_G, \vec{B}_G) \rightarrow$

$$
\begin{aligned}
\vec{\nabla} \cdot \vec{E}_G &= -4\pi G \rho \\
\vec{\nabla} \cdot \vec{B}_G &= 0 \\
\vec{\nabla} \wedge \vec{E}_G &= -\frac{1}{2c}\frac{\partial}{\partial t}\vec{B}_G \\
\vec{\nabla} \wedge \vec{B}_G &= \frac{2}{c}\frac{\partial}{\partial t}\vec{E}_G - \frac{8\pi G}{c}\vec{j} \\
\vec{E}_G &= -\vec{\nabla}\Phi - \frac{1}{2c}\frac{\partial}{\partial t}\vec{A} \\
\vec{B}_G &= \vec{\nabla} \wedge \vec{A} \\
\frac{1}{c}\frac{\partial}{\partial t}\Phi + \frac{1}{2}\vec{\nabla} \cdot \vec{A} &= 0
\end{aligned}
$$

ρ = mass-charge density

j = mass-current density

The Lense-Thirring effect and gravitomagnetism

Gravito-electromagnetism: linearized theory of General Relativity (GR)

In the Weak-Field and Slow-Motion (**WFSM**) limit of the theory of **GR**, Einstein's equations reduce to a form quite similar to those of electromagnetism. Following this approach we have a:

- gravitoelectric field produced by masses, analogous to the electric field produced by charges
- gravitomagnetic field produced by mass currents, analogous to the magnetic field produced by electric currents.

$$G_{\alpha\beta} = 8\pi \frac{G}{c^4} T_{\alpha\beta}$$

$$\eta_{\alpha\beta} = \begin{pmatrix} 1 & 0 & 0 & 0 \\ 0 & -1 & 0 & 0 \\ 0 & 0 & -1 & 0 \\ 0 & 0 & 0 & -1 \end{pmatrix}$$

$$\begin{cases} \bar{h}^{\alpha\beta}{}_{,\beta} = 0 \\ g_{\alpha\beta} = \eta_{\alpha\beta} + h_{\alpha\beta} \\ \Delta \bar{h}_{\alpha\beta} = 16\pi \frac{G}{c^4} T_{\alpha\beta} \end{cases}$$

$$\begin{cases} \bar{h}_{\alpha\beta} \equiv h_{\alpha\beta} - \frac{1}{2}\eta_{\alpha\beta} h \\ h \equiv h^{\alpha}_{\alpha} = \eta^{\alpha\beta} h_{\alpha\beta} \end{cases}$$

$$|h_{\alpha\beta}| \cong \left|\frac{\Phi}{c^2}\right| \leq 10^{-6}$$

$$\begin{cases} \bar{h}^{00} = 4\frac{\Phi}{c^2} \\ \bar{h}^{0l} = -2\frac{A^l}{c^2} \\ \bar{h}^{ij} = O\left(c^{-4}\right) \end{cases}$$

$$\Phi = -\frac{GM_\odot}{R_\odot}$$

Gravitoelectric potential

$$A^l = \frac{G}{c}\frac{J^n x^k}{r^3}\varepsilon^l_{nk}$$

Gravitomagnetic potential

The Lense-Thirring effect and gravitomagnetism

Formal analogy with electrodynamics: linearized theory of General Relativity (WFSM limit)

Classical Electrodynamics:

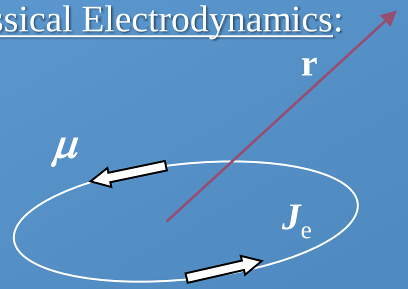

$\boldsymbol{A}(\mathbf{r})$

$\boldsymbol{B}(\mathbf{r})$

Classical Geometrodynamics (WFSM):

G = c = 1

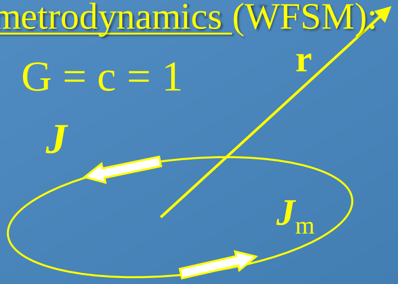

$\boldsymbol{h}(\mathbf{r})$

$\boldsymbol{B_G}(\mathbf{r})$

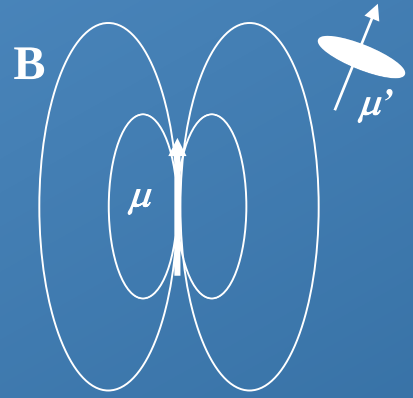

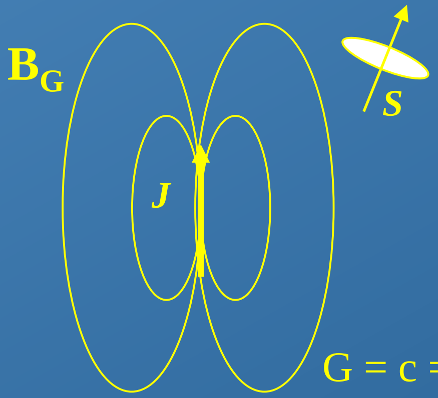

$$\Delta\vec{A} = -4\pi\cdot\vec{J}_e \qquad\qquad \Delta\vec{h} = 16\pi\cdot\vec{J}_m$$

solution:

$$\vec{A}(\vec{r}) = \int\frac{\vec{J}_e(\vec{r}\,')}{|\vec{r}-\vec{r}\,'|}d^3r' \qquad\qquad \vec{h}(\vec{r}) = -4\int\frac{\vec{J}_m(\vec{r}\,')}{|\vec{r}-\vec{r}\,'|}d^3r'$$

$$\vec{\mu} = \tfrac{1}{2}\int\vec{r}\wedge\vec{J}_e(\vec{r})d^3r \qquad\qquad \vec{J} = \int\vec{r}\wedge\vec{J}_m(\vec{r})d^3r$$

$$\vec{A}(\vec{r}) \cong \frac{\vec{\mu}\wedge\vec{r}}{r^3} \qquad\qquad \vec{h}(\vec{r}) \cong -2\frac{\vec{J}\wedge\vec{r}}{r^3}$$

$$\vec{B} = \vec{\nabla}\wedge\vec{A} \cong \frac{3\hat{r}(\hat{r}\bullet\vec{\mu})-\vec{\mu}}{r^3} \qquad\qquad \vec{B}_G = \vec{\nabla}\wedge\vec{h} \cong -2\frac{3\hat{r}(\hat{r}\bullet\vec{J})-\vec{J}}{r^3}$$

$$\boxed{\vec{F} = m\ddot{\vec{r}} = q(\vec{E}+\dot{\vec{r}}\wedge\vec{B})} \qquad\qquad \boxed{\vec{F} = m\ddot{\vec{r}} = m(-\frac{M}{r^2}\hat{r}+\dot{\vec{r}}\wedge\vec{B}_G)}$$

$$\vec{F} = (\vec{\mu}'\bullet\vec{\nabla})\vec{B} \qquad\qquad \vec{F} = \frac{1}{2}(\vec{S}\bullet\vec{\nabla})\vec{B}_G$$

$$\vec{N} = \vec{\mu}'\wedge\vec{B} \qquad\qquad \vec{N} = \frac{1}{2}\vec{S}\wedge\vec{B}_G$$

$$\dot{\vec{\Omega}} = -\vec{B} = \frac{\vec{\mu}-3\hat{r}(\hat{r}\bullet\vec{\mu})}{r^3} \qquad\qquad \dot{\vec{\Omega}} = -\frac{1}{2}\vec{B}_G = \frac{-\vec{J}+3\hat{r}(\hat{r}\bullet\vec{J})}{r^3}$$

This phenomenon is known as dragging of gyroscopes or dragging of inertial frames

Therefore, mass currents (as the rotating Earth) drag gyroscopes and change the orientation of their axes

The Lense-Thirring effect and gravitomagnetism

The so-called Lense-Thirring effect (1918) is a consequence of the Gravitomagnetic field of the Earth produced by its rotation, i.e. by its Angular Momentum:

$$\left\langle \frac{d\Omega}{dt} \right\rangle_{sec} = \frac{2G}{c^2 a^3} \frac{J_\oplus}{(1-e^2)^{3/2}}$$

$$\left\langle \frac{d\omega}{dt} \right\rangle_{sec} = -\frac{6G}{c^2 a^3} \frac{J_\oplus}{(1-e^2)^{3/2}} \cos i$$

Lense-Thirring, Phys. Z, 19, 1918

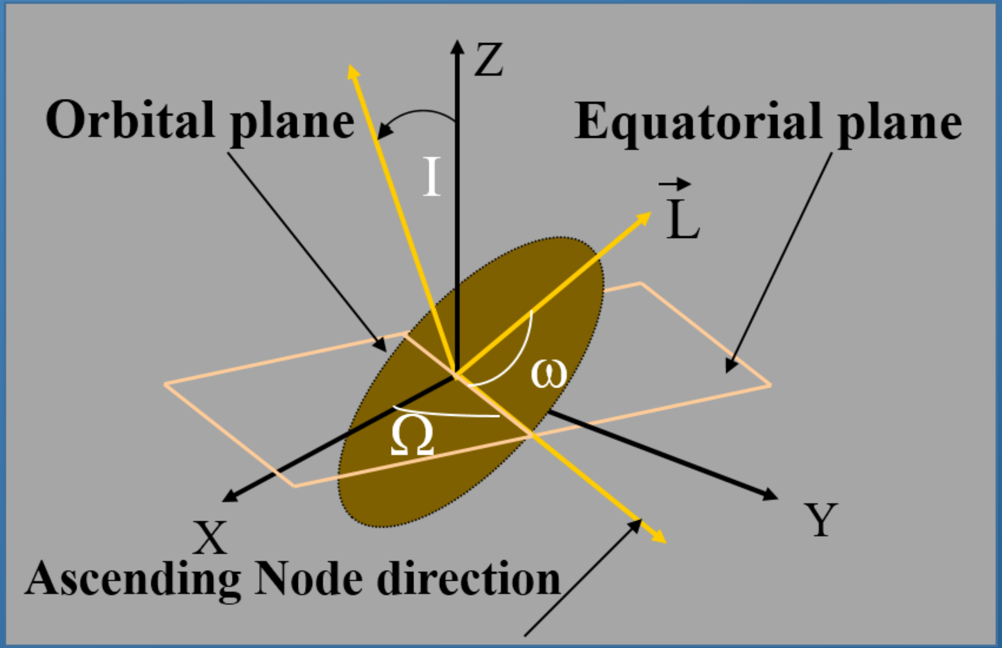

These are the results of the frame–dragging effect or Lense–Thirring effect:

moving masses (i.e., mass–currents) are rotationally dragged by the angular momentum of the primary body (mass–current)

The LARASE experiment and its goals

The LAser RAnged Satellites Experiment (LARASE) goals:

- The main goal is to provide accurate measurements for the gravitational interaction in the **weak-field** and **slow-motion** limit of **General Relativity** by means of a very precise laser tracking of geodetic satellites orbiting around the Earth (the two **LAGEOS** and **LARES**)
- Beside the quality of the tracking observations, guaranteed by the powerful **Satellite Laser Ranging** (**SLR**) technique of the **International Laser Ranging Service** (**ILRS**), also the quality of the dynamical models implemented in the **Precise Orbit Determination** (**POD**) software plays a fundamental role in order to obtain precise and accurate measurements
- The models have to account for the perturbations due to both gravitational and non-gravitational forces in such a way to reduce as much as possible the difference between the *observed* range, from the tracking, and the *computed* one, from the models
- In particular, **LARASE** aims to improve the dynamical models of the current best laser-ranged satellites in order to perform a precise and accurate orbit determination, able to benefit also space geodesy and geophysics

LAser **RE**lativity **S**atellite

The LARASE experiment and its goals

LAGEOS, LAGEOS II and LARES

orbit, size, mass and materials

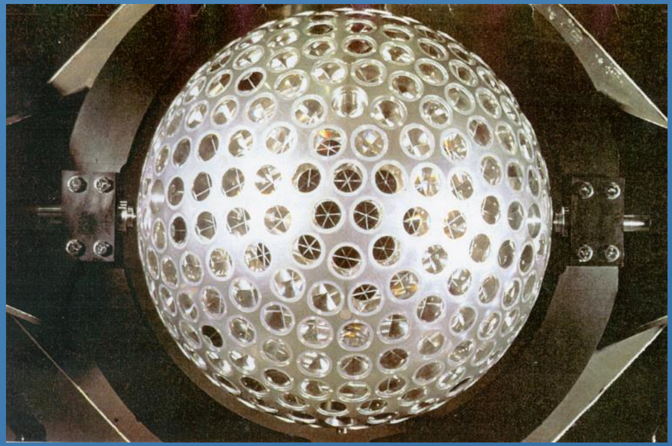

LAser **GEO**dynamic **S**atellite
LAGEOS II

LAGEOS (NASA 1976)
LAGEOS II (NASA/ASI 1992)
LARES (ASI 2012)

Parameter		LARES	LAGEOS	LAGEOS II
a	[km]	7 820	12 270	12 163
e		0.001	0.004	0.014
I	[deg]	69.5	109.8	52.7
R	[cm]	18.2	30	30
M	[kg]	386.8	406.9	405.4
A/M	[m2/kg]	$2.69 \cdot 10^{-4}$	$6.94 \cdot 10^{-4}$	$6.97 \cdot 10^{-4}$

$$\left.\frac{A}{M}\right|_{Lares} \cong \frac{1}{2.6}\left.\frac{A}{M}\right|_{Lageos}$$

	LARES	LAGEOS
material	Tungsten	Al/Brass/Be/Cu
CCR (suprasil 311)	92	422 + 4
bin	30 s	120 s

The LARASE experiment and its goals

The LARASE activities:

1. Review of the literature, technical notes and all the documentation (**NASA**, **ALENIA**, **ASI**) related with the structure of the satellites and their physical characteristics
2. A reconstruction of the internal and external structure of the satellites with finite elements techniques
3. New spin model for the two **LAGEOS** satellites and **LARES** accounting of their complex interaction with the Earth's magnetic field: **LASSOS** (**LA**rase **S**atellites **S**pin m**O**del **S**olutions)
4. New models for the thermal thrust perturbations, also with a Finite Element Model (FEM)
5. Impact of the neutral drag on the two **LAGEOS** satellites and on **LARES**
6. Precise Orbit Determination for the two **LAGEOS** satellites and for **LARES**
7. Solid and Ocean tides on the two **LAGEOS** satellites and on **LARES**
8. Gravitational perturbations with estimate of the spherical harmonics (SH) of low degree
9. Fundamental Physics measurements

The LARASE experiment and its goals

Some results: moments of inertia and internal structure

Table 1. Principal moments of inertia of LAGEOS, LAGEOS II and LARES in their flight arrangement.

Satellite	Moments of inertia (kg m^2)		
	I_{zz}	I_{xx}	I_{yy}
LAGEOS	11.42 ± 0.03	10.96 ± 0.03	10.96 ± 0.03
LAGEOS II	11.45 ± 0.03	11.00 ± 0.03	11.00 ± 0.03
LARES	4.77 ± 0.03	4.77 ± 0.03	4.77 ± 0.03

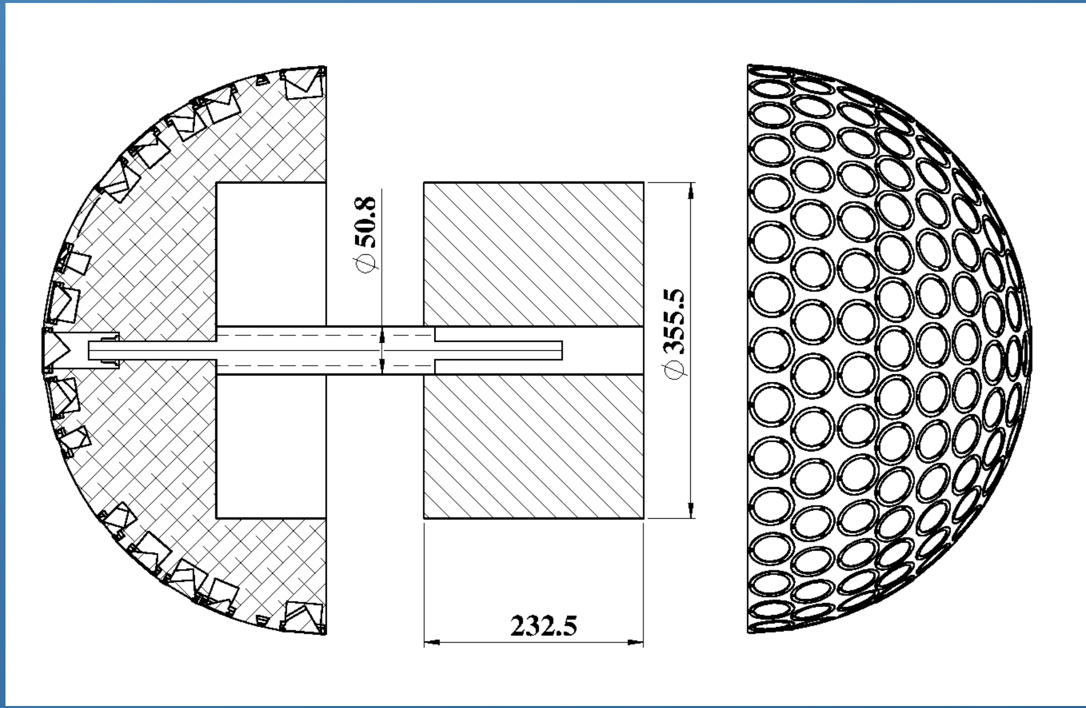

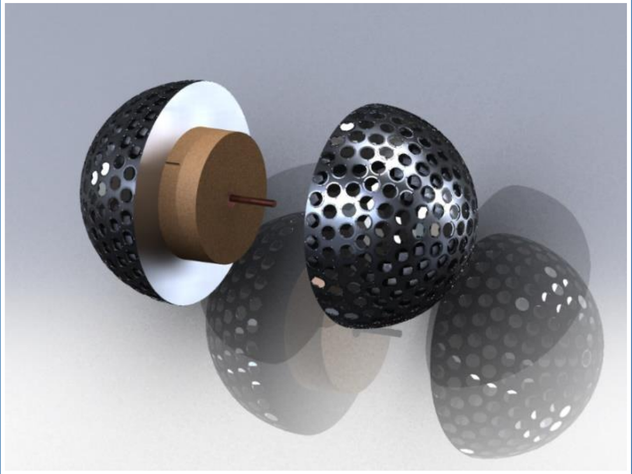

- The core is made of BRASS
- The stud is made of BERYLLIUM and COPPER

The LASSOS model for the spin

Spin Models

The rotational dynamics of a satellite represents a very important issue that deeply impacts the goodness of the orbit modelling

Indeed, the modelling of several disturbing effects (like the thermal thrust ones) depends on the knowledge of the spin period and orientation in the inertial space:

1. Yarkovsky–Schach effect
2. Earth–Yarkovsky (Rubincam) effect
3. Asymmetric reflectivity from the satellite surface

Their modelling will greatly improve the POD of the two LAGEOS satellites avoiding the current (and significant) use of empirical accelerations during the data reduction

The LASSOS model for the spin

Past Spin Models

The best spin models developed in the past are:

1. Bertotti and Iess (JGR 96 B2, 1991)
2. Habib et al. (PRD 50, 1994)
3. Farinella, Vokrouhlicky and Barlier (JGR 101, 1996); Vokrouhlicky (GRL 23, 1996)
4. Andrés, 1997 (PhD Thesis) and LOSSAM

All of these studies, with the exception of Habib et al., attack and solve the problem of the evolution of the rotation of a satellite in a terrestrial inertial reference system, in the so-called rapid spin approximation and they introduce equations for the external torques that are averaged over time; their fit to the spin observations was good, especially in the case of the LOSSAM model for the LAGEOS II satellite. Habib et al. use a body-fixed reference system and non-averaged torques; their model does not fit so well the observations

The LASSOS model for the spin

LARASE Spin Model LASSOS (LArase Satellites Spin mOdel Solutions)

We have deeply reviewed previous spin models, in particular we:

- first built our own spin model in the rapid spin approximation
- adopted non-averaged torques in the equations to describe the slow spin approximation: we solved the problem of a metallic sphere rotating in an alternate magnetic field
- introduced in the equations all known possible torques (like in LOSSAM model)
- solved the equations in a body-fixed reference system in order to better describe the misalignment between the symmetry axis and the spin
- included in the equations the terms due to the transversal asymmetry
- carefully studied the satellites moments of inertia

The LARASE experiment and its goals

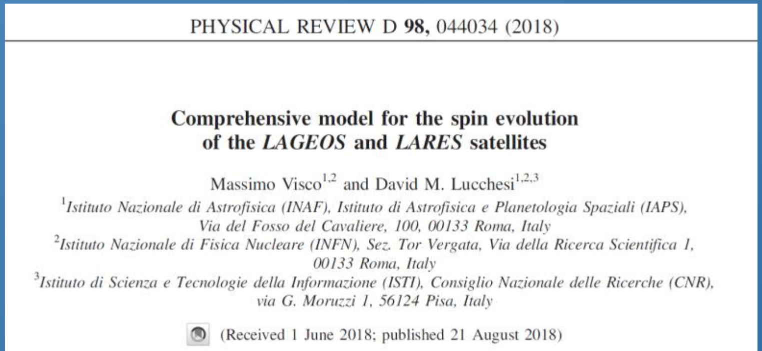
PHYSICAL REVIEW D 98, 044034 (2018)

Comprehensive model for the spin evolution of the *LAGEOS* and *LARES* satellites

Massimo Visco[1,2] and David M. Lucchesi[1,2,3]
[1]*Istituto Nazionale di Astrofisica (INAF), Istituto di Astrofisica e Planetologia Spaziali (IAPS), Via del Fosso del Cavaliere, 100, 00133 Roma, Italy*
[2]*Istituto Nazionale di Fisica Nucleare (INFN), Sez. Tor Vergata, Via della Ricerca Scientifica 1, 00133 Roma, Italy*
[3]*Istituto di Scienza e Tecnologie della Informazione (ISTI), Consiglio Nazionale delle Ricerche (CNR), via G. Moruzzi 1, 56124 Pisa, Italy*

(Received 1 June 2018; published 21 August 2018)

LARASE Spin Model: results for LAGEOS II

LArase **S**atellites **S**pin m**O**del **S**olutions (**LASSOS**)

Blue = LARASE model for the rapid-spin
Red = LARASE general model

Spin Orientation: α, δ

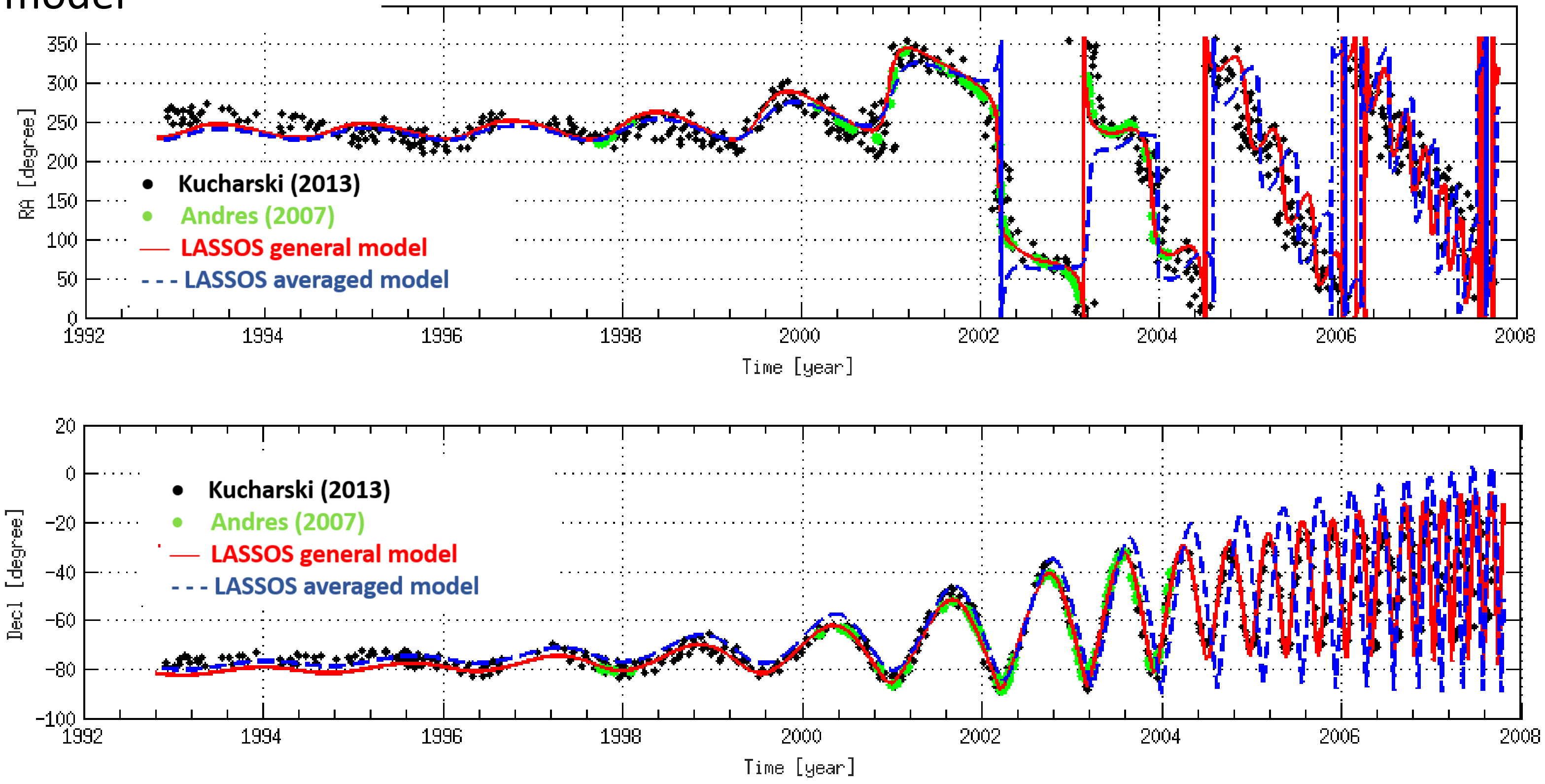

The LARASE experiment and its goals

LARASE Spin Model: results for LAGEOS II

LArase **S**atellites **S**pin m**O**del **S**olutions (**LASSOS**)

PHYSICAL REVIEW D **98,** 044034 (2018)

Comprehensive model for the spin evolution of the *LAGEOS* and *LARES* satellites

Massimo Visco[1,2] and David M. Lucchesi[1,2,3]

[1]*Istituto Nazionale di Astrofisica (INAF), Istituto di Astrofisica e Planetologia Spaziali (IAPS), Via del Fosso del Cavaliere, 100, 00133 Roma, Italy*
[2]*Istituto Nazionale di Fisica Nucleare (INFN), Sez. Tor Vergata, Via della Ricerca Scientifica 1, 00133 Roma, Italy*
[3]*Istituto di Scienza e Tecnologie della Informazione (ISTI), Consiglio Nazionale delle Ricerche (CNR), via G. Moruzzi 1, 56124 Pisa, Italy*

(Received 1 June 2018; published 21 August 2018)

Blue = LARASE model for the rapid-spin
Red = LARASE general model

Rotational Period: P

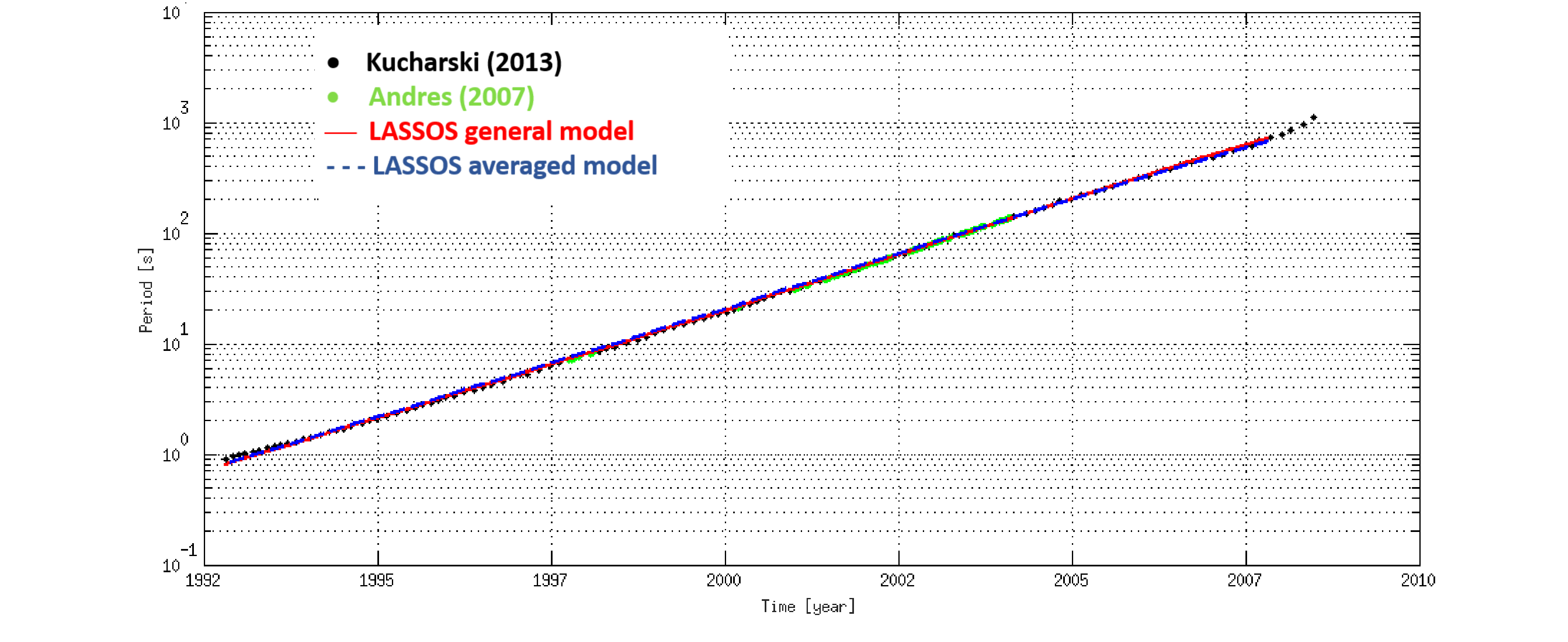

Thermal effects and their modelling

An intricate role, among the complex non-gravitational perturbations, is played by the subtle thermal thrust effects that arise from the radiation emitted from the satellite surface as consequence of the non uniform distribution of its temperature

In the literature of the older LAGEOS satellite this problem was attacked since the early 80s' of the past century to explain the (apparently) anomalous behavior of the along-track acceleration of the satellite, characterized by a complex pattern:

Rubincam, Afonso, Ries, Scharroo, Farinella, Metris, Vokrouhlicky, Slabinsky, Lucchesi, Andres, …

represents a non exhaustive list of the researchers that have successfully worked on this very important issue

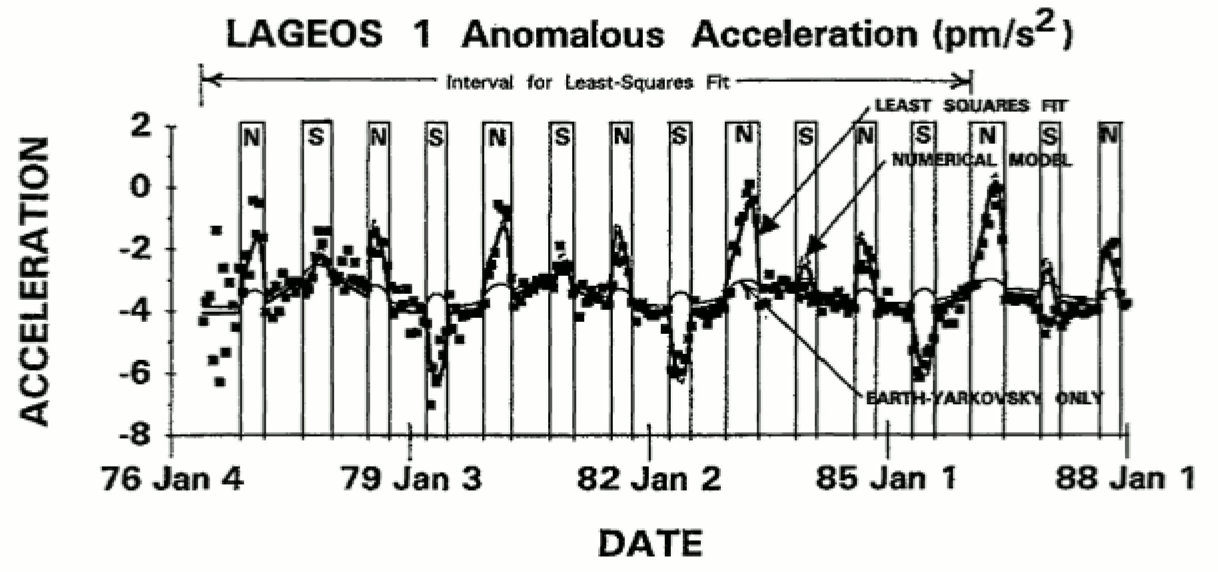

Figure 2. LAGEOS 1 anomalous acceleration: observed data points (squares) are based on 15 day fits to laser data by the Center for Space Research, University of Texas at Austin. The vertical bars mark eclipse seasons. N at top of bar denotes season when satellite travels northward through earth shadow; S denotes season with southward travel.

Thermal effects and their modelling

The dynamical problem to solve is quite complex and should account of the following main aspects:

- A deep physical characterization of the satellite
  - emission and absorption coefficients, thermal conductivity, heat capacity, thermal inertia, …
- Rotational dynamics of the satellite
  - Spin orientation and rate
- Radiation sources
  - Sun and Earth

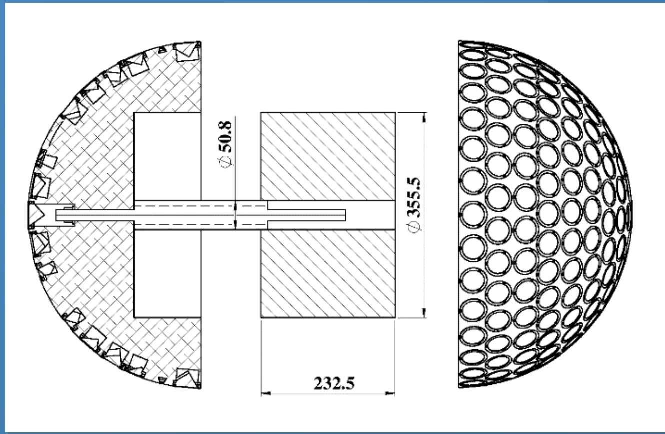

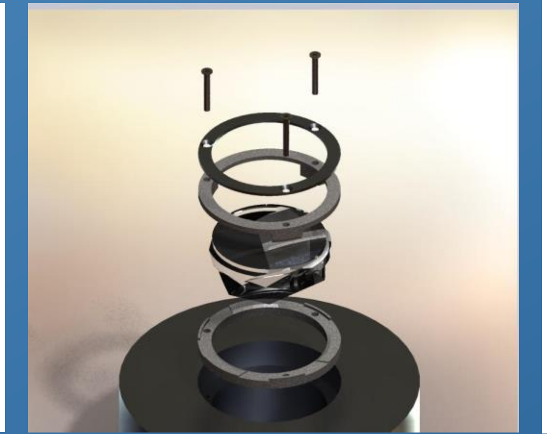

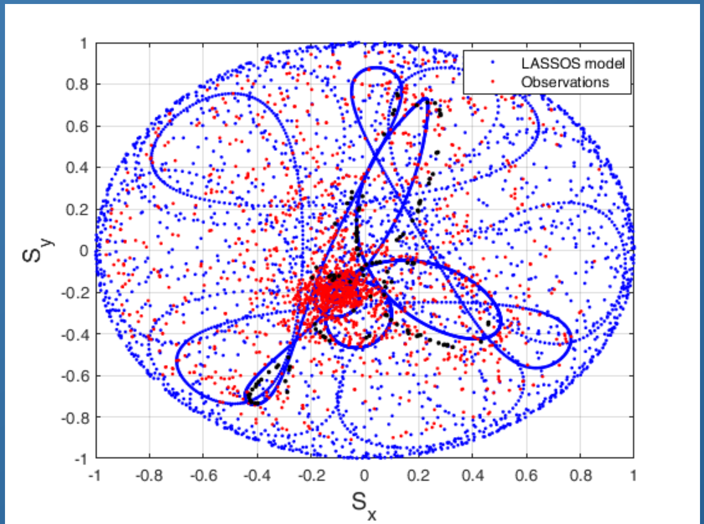

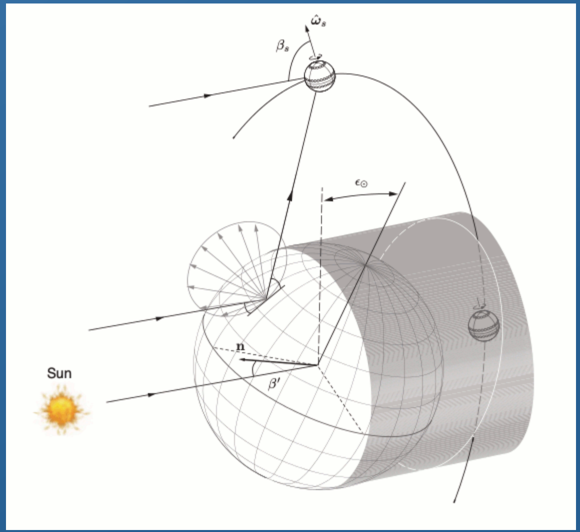

Thermal effects and their modelling

We have tackled the problem following the two approaches considered in the past in the literature (but with some differences):

- We developed a simplified thermal model of the satellite based on
  - the energy balance equation on its surface
  - a linear approach for the distribution of the temperature with respect to its equilibrium (mean) temperature

- A general thermal model based on
  - a satellite (metallic structure) in thermal equilibrium
  - the CCRs rings are at the same temperature of the satellite
  - for each CCR the thermal exchange with the satellite is computed

$$\frac{dQ_i}{dt} \cong \sum_j (P_j - \boxed{\varepsilon_j \sigma A_{ext,j} T_i^4}) + \sum_k \boxed{R_{i,k}\left(T_k^4 - T_i^4\right)} + \sum_k \boxed{C_{i,k}(T_k - T_i)} + \cdots = \mathcal{H}_i \frac{\partial T_i}{\partial t}$$

Absorbed power

Emitted power

Power exchanged by radiation

Power exchanged by conduction

Thermal effects and their modelling

The main perturbations to be taken into account are:

- The solar Yarkovsky-Schach effect
  - an anisotropic emission of thermal radiation that arises from the temperature gradients across the surface produced by the solar heating and the thermal inertia of the various parts (mainly from the CCRs)
  - it produces long-term effects when the thermal radiation is modulated by the eclipses
- The Earth Yarkovsky thermal (or Rubincam) effect
  - the temperature gradients responsible of the anisotropic emission of thermal radiation are produced by the Earth's infrared radiation
  - the bulk of the effect is due to the CCRs and their thermal inertia
- The asymmetric reflectivity effect

In the following only the Yarkovsky-Schach effect will be considered

Thermal effects and their modelling

In case of a simplified thermal model we can skip the details of a complete characterization of the satellite thermal behavior. What really matters are:

- The satellite mean temperature
  - T_0
- The temperature difference between the CCRs of the hemisphere facing the Sun with respect to those in the dark side
  - ΔT
- The CCRs thermal inertia
  - τ

- In the following the results for the LAGEOS II satellite are shown
- The LASSOS (LArase Satellites Spin mOdel Solutions) general spin model has been used

Thermal effects and their modelling

Analysis performed for the Yarkovsky-Schach effect:

- We run our routine over a 20 years time span from MJD 48932, i.e. Nov. 6^{th} 1992, and we computed the effects on the orbit elements of LAGEOS II
- We compared the results with the residuals in the satellite orbit elements that we obtained from a POD with GEODYN II:
    - Background gravity model: EIGEN-GRACE02S
    - Arc length of 7 days
    - No empirical accelerations
    - Thermal effects (Yarkovsky Schach and Rubincam) not modelled
    - General relativity modelled with the exception of the Lense-Thirring effect

Thermal effects and their modelling

Orbit perturbation and comparison with the residuals: semi-major axis

$$\frac{da}{dt} = \frac{2}{n\sqrt{1-e^2}}[T + e(T\cos f + R\sin f)]$$

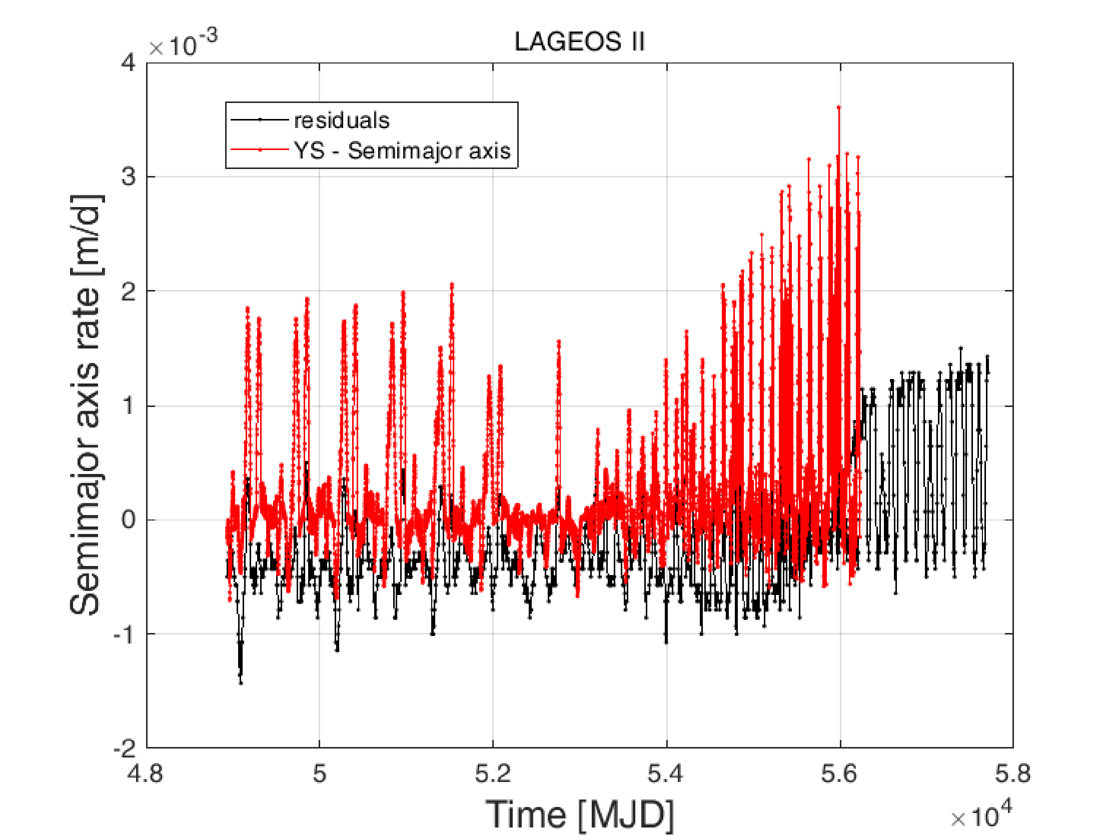

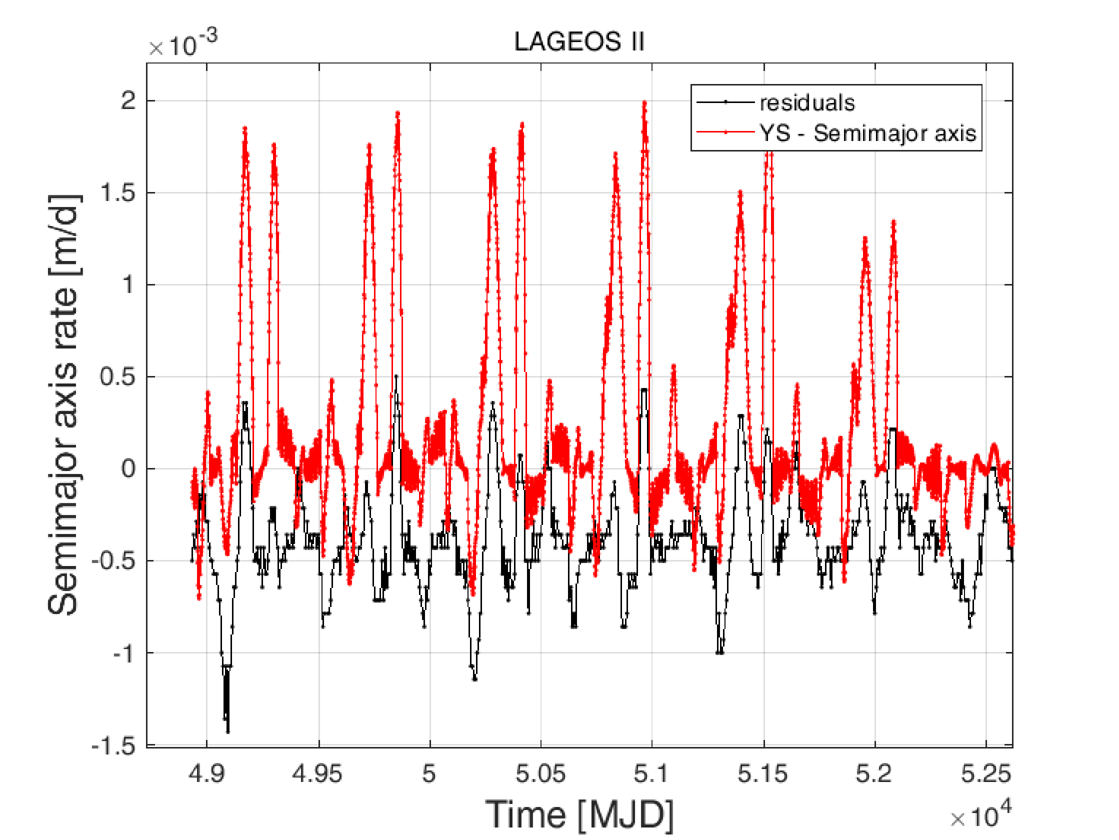

Thermal effects and their modelling

Orbit perturbation and comparison with the residuals: eccentricity

$$\frac{de}{dt} = \frac{\sqrt{1-e^2}}{na}\left[R\sin f + T(\cos f + \cos u)\right]$$

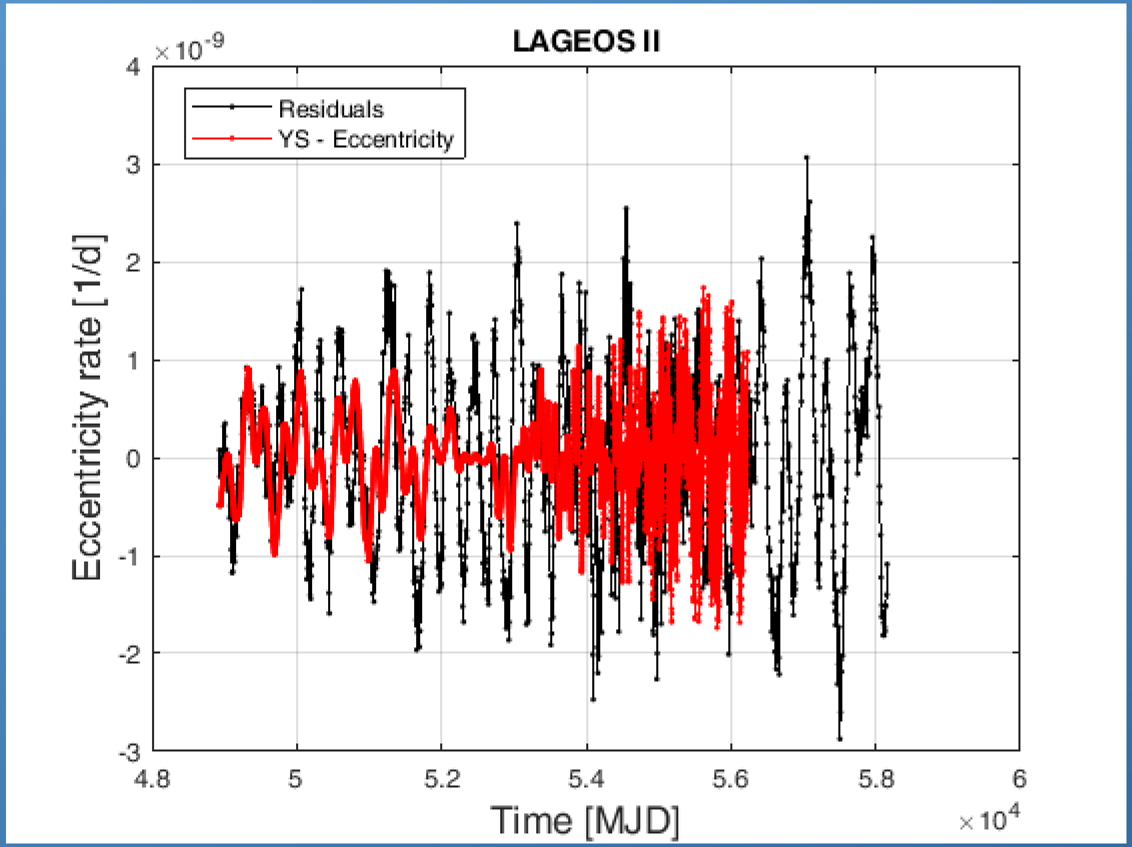

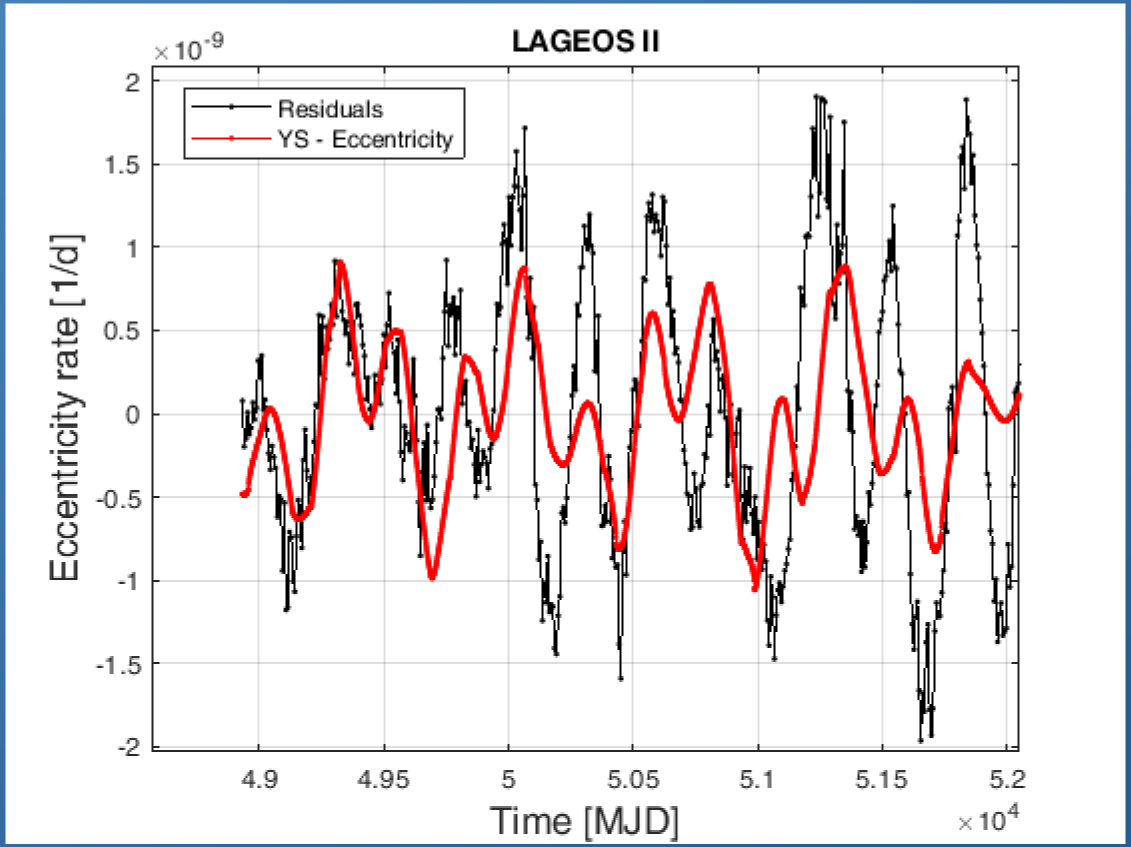

Thermal effects and their modelling

Orbit perturbation and comparison with the residuals: argument of pericenter

$$\frac{d\omega}{dt} = \frac{\sqrt{1-e^2}}{nea}\left[-R\cos f + T\left(\sin f + \frac{1}{\sqrt{1-e^2}}\sin u\right)\right] - \frac{W}{na^2\sqrt{1-e^2}}\frac{1}{\tan i}r\sin(\omega + f)$$

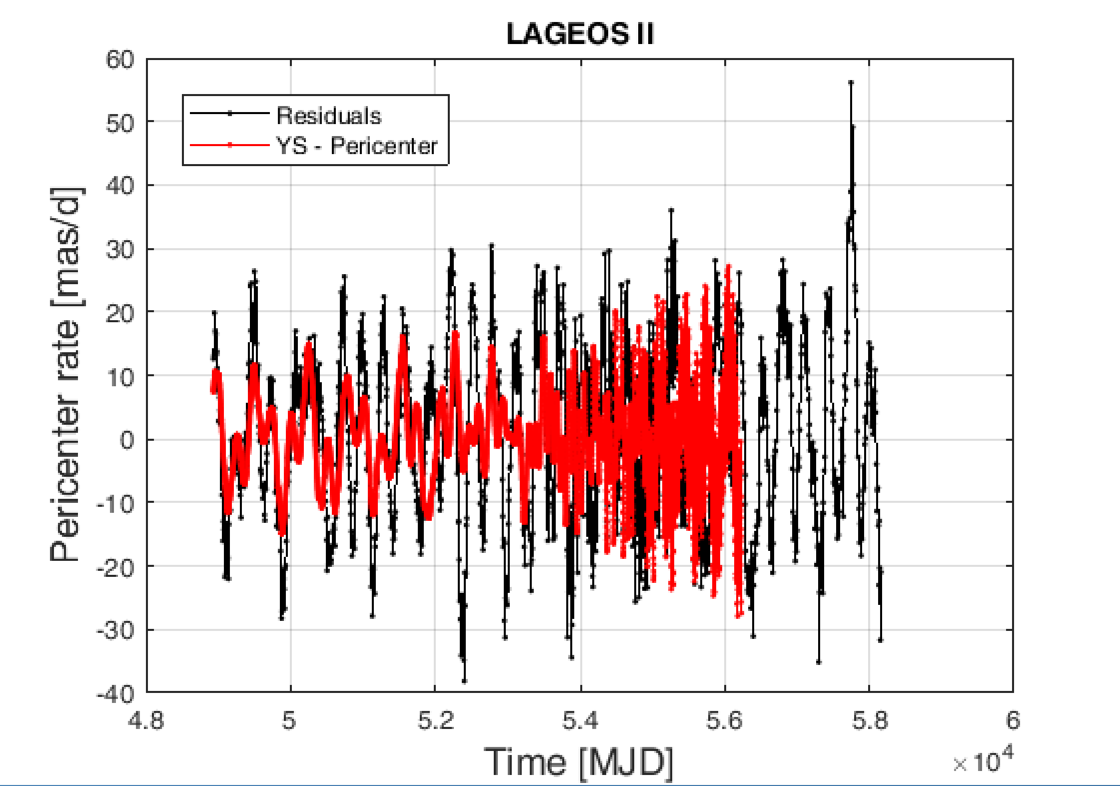

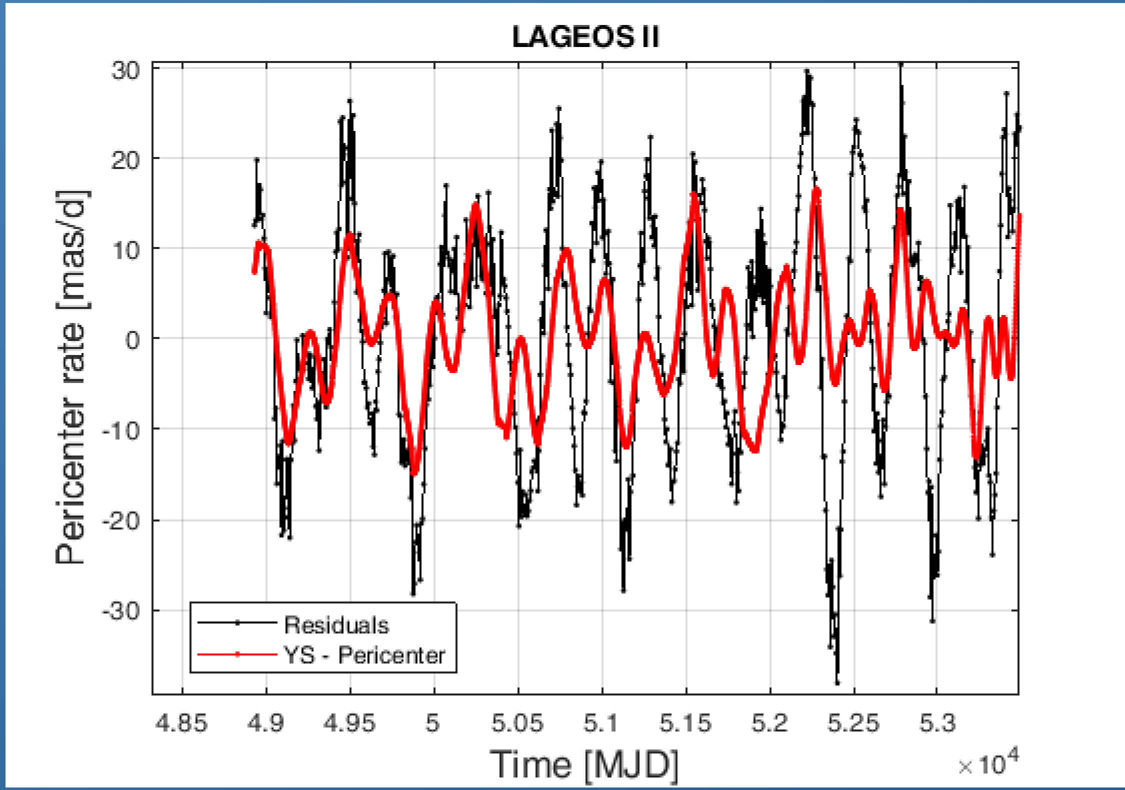

Thermal effects and their modelling

Preliminary comparison between the simplified and the general thermal model

Accelerations in Gauss co-moving frame

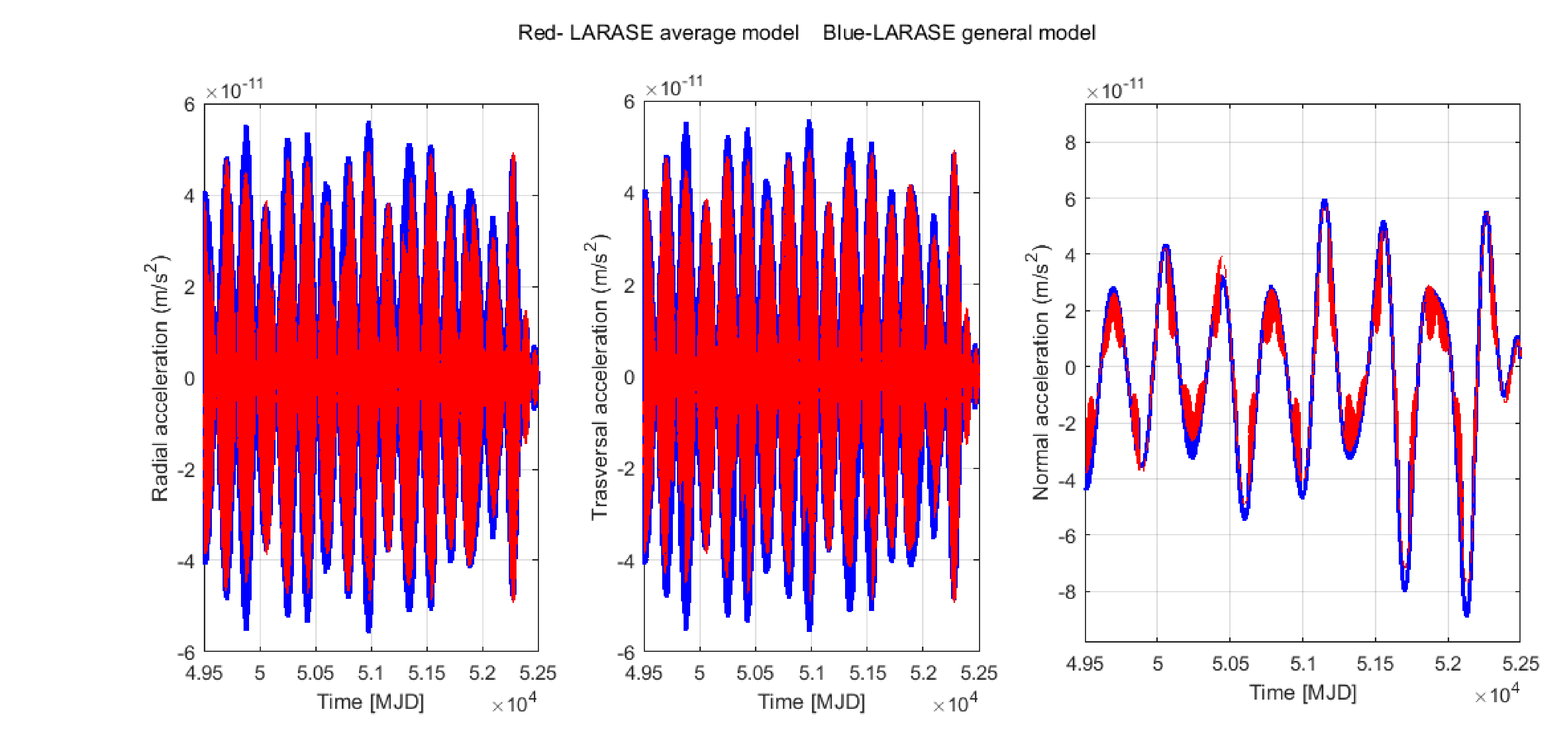

Thermal effects and their modelling

Preliminary comparison between the simplified and the general thermal model

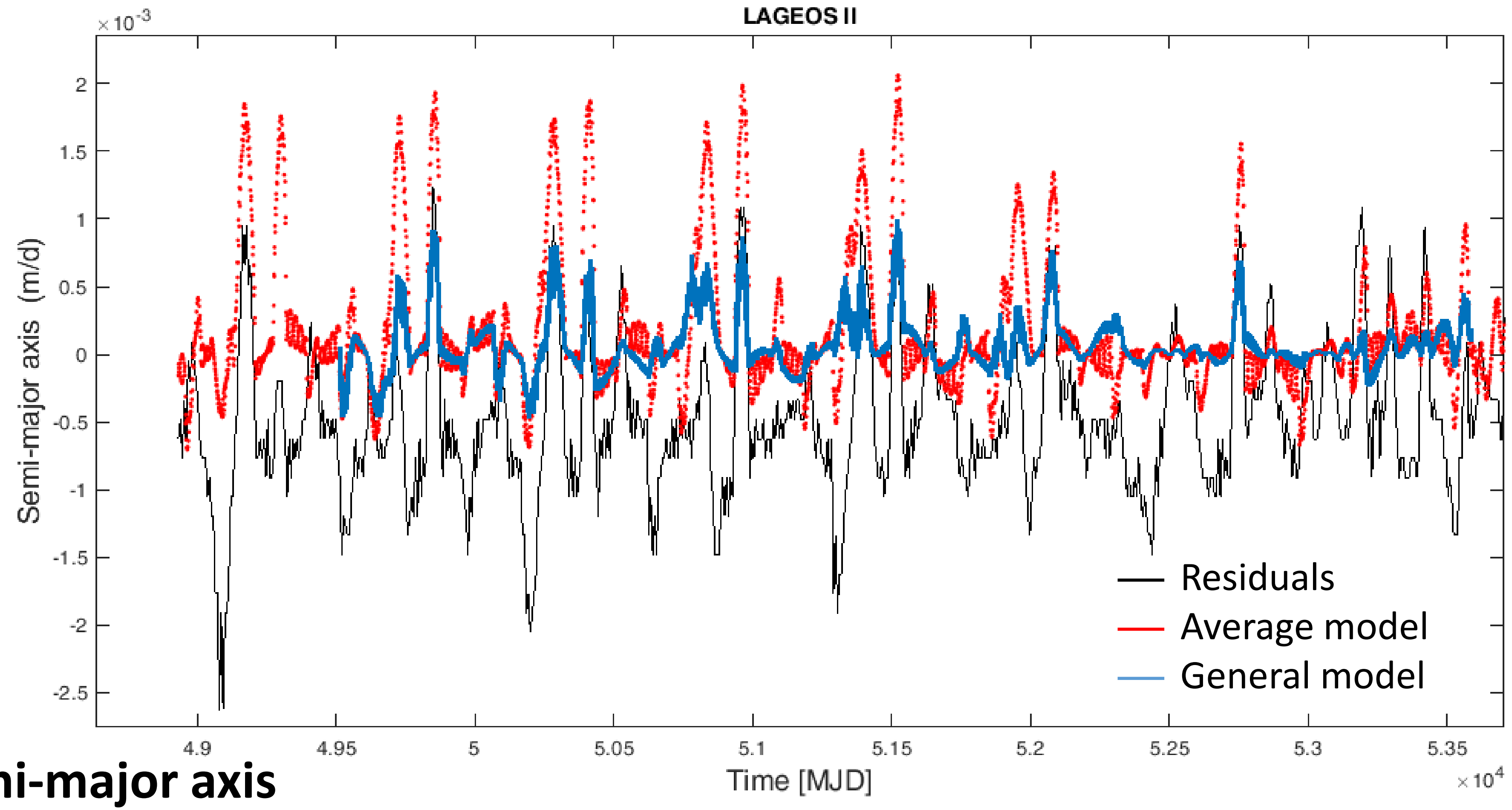

Semi-major axis

Thermal effects and their modelling

Preliminary comparison between the simplified and the general thermal model

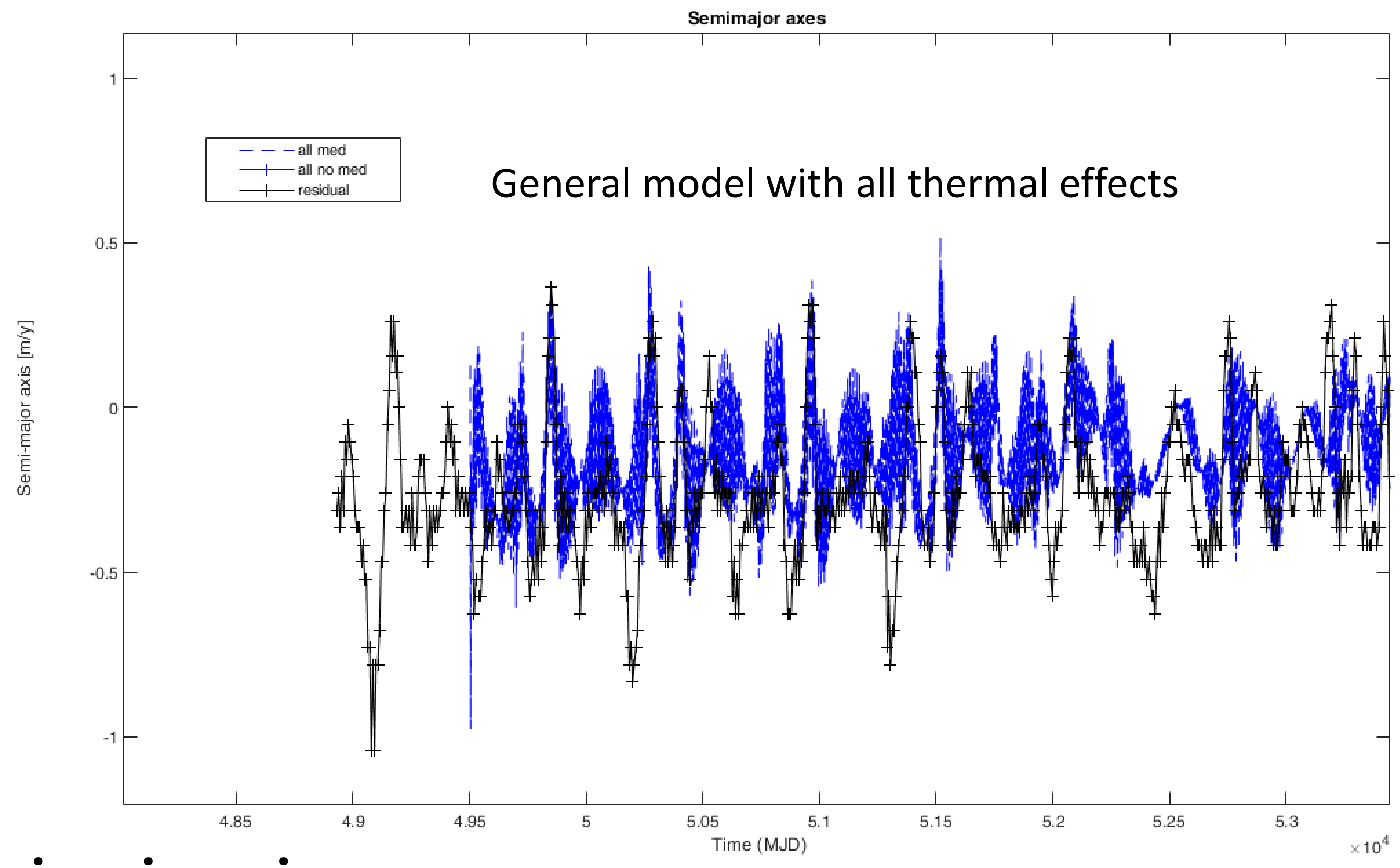

Semi-major axis

Thermal effects and their modelling

Preliminary comparison between the simplified and the general thermal model

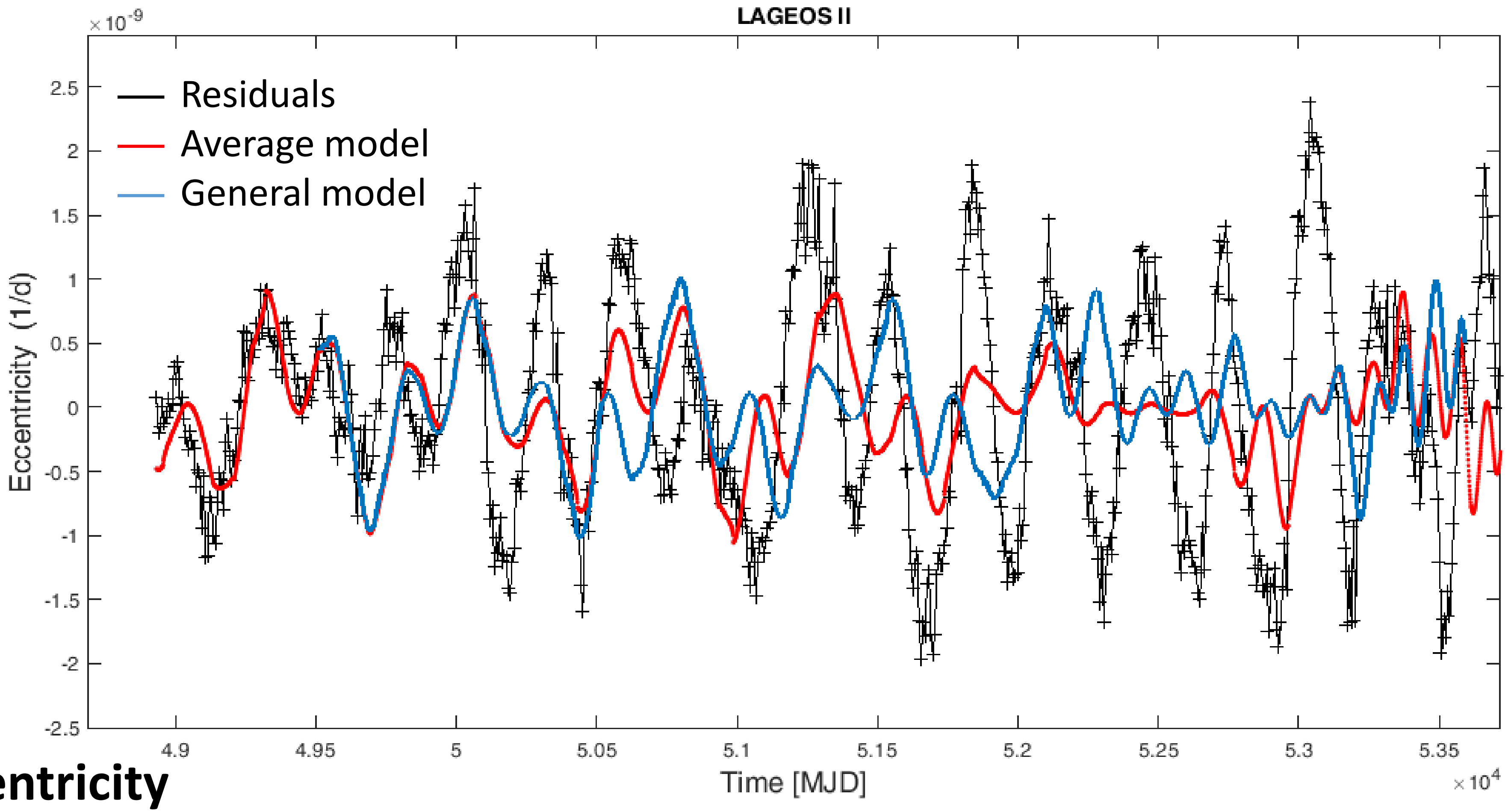

Eccentricity

Thermal effects and their modelling

Preliminary comparison between the simplified and the general thermal model

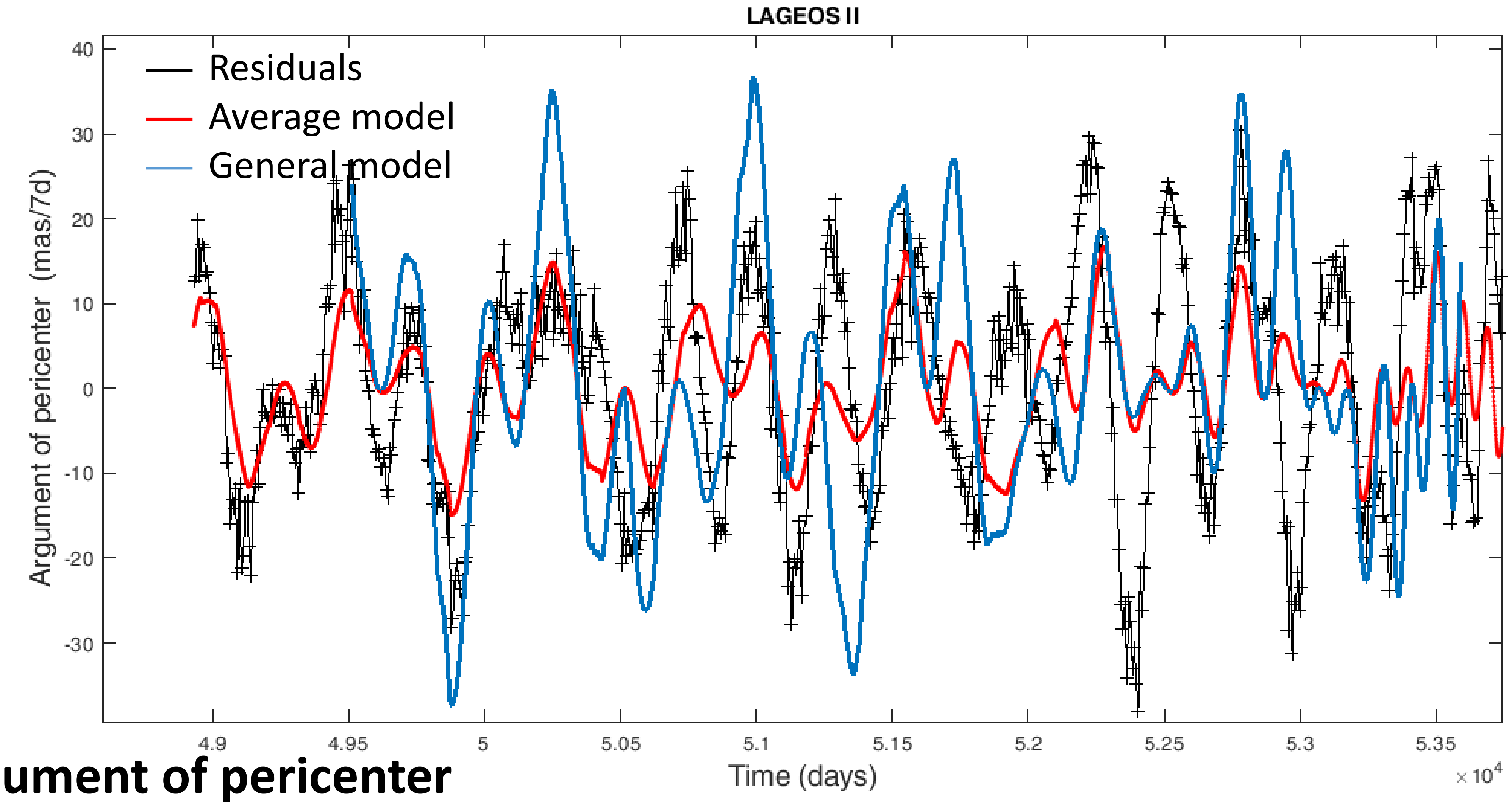

Argument of pericenter

Model for the Earth's gravitational field

The correct knowledge of the Earth's gravitational field impacts significantly on the Lense-Thirring effect measurement:

$$\langle \dot{\Omega}_{LT} \rangle_{sec} = \frac{2G}{c^2 a^3} \frac{J_\oplus}{(1-e^2)^{3/2}}$$

$$U = -\frac{GM_\oplus}{r} \sum_{\ell=0}^{\infty} \sum_{m=0}^{\ell} \left(\frac{R_\oplus}{r}\right)^{\ell} P_{\ell m}(\sin\varphi)\Big(C_{\ell m}\cos m\lambda + S_{\ell m}\sin m\lambda\Big),$$

$$\langle \dot{\Omega}_{class} \rangle_{sec} = -\frac{3}{2} n \left(\frac{R_\oplus}{a}\right)^2 \frac{\cos i}{(1-e^2)^2} \{-\sqrt{5}\bar{C}_{20}\} + \cdots$$

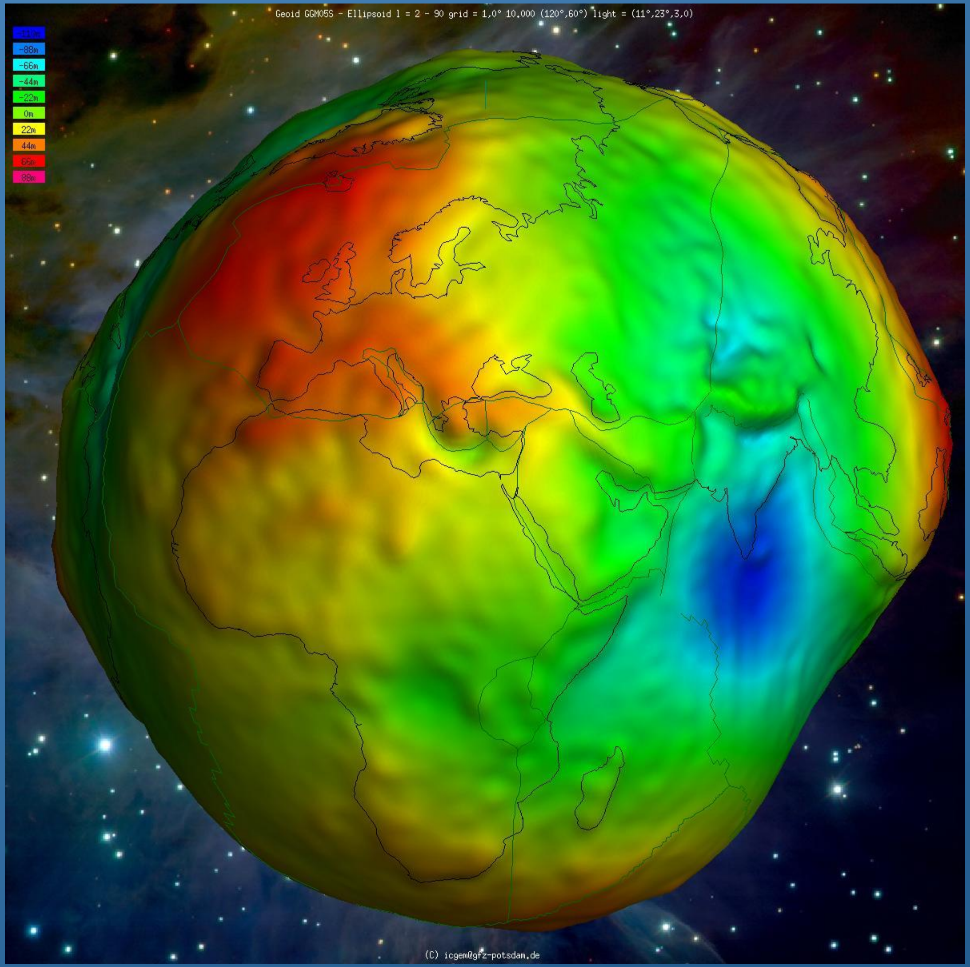

with important (possible) systematic effects…

ℓ = even and m = 0

Model for the Earth's gravitational field

The magnitude of the effect to be measured

$$\langle \dot{\Omega}_{LT} \rangle_{sec} = \frac{2G}{c^2 a^3} \frac{J_\oplus}{(1-e^2)^{3/2}}$$

Table 3. Mean orbital elements of LAGEOS, LAGEOS II and LARES.

Element	Unit	Symbol	LAGEOS	LAGEOS II	LARES
Semi-major axis	[km]	a	12 270.00	12 162.07	7 820.31
Eccentricity		e	0.004433	0.013798	0.001196
Inclination	[deg]	i	109.84	52.66	69.49

$$\begin{cases} G \cong 6.670 \cdot 10^{-8}\, cm^3 s^{-2} g^{-1} \\ J_\oplus \cong 5.861 \cdot 10^{40}\, cm^2 g s^{-1} \\ c \cong 2.9979250 \cdot 10^{10}\, cm/s \end{cases}$$

TABLE II. Rate in milli-arc-sec per year (mas/yr) for the secular Lense-Thirring precession on the right ascension of the ascending node of the two LAGEOS and LARES satellites.

Orbital element	LAGEOS	LAGEOS II	LARES
$\dot{\Omega}^{LT}$	30.67	31.50	118.48

30 mas ≅ 1.8 m

The effect on the orbit is quite small

Total precession:

$$\dot{\Omega}^{Obser}_{Lageos} \cong +126^\circ / yr \qquad \dot{\Omega}^{Obser}_{LageosII} \cong -231^\circ / yr$$

Model for the Earth's gravitational field

By solving a linear system of three equations in three unknowns, we can solve for the relativistic precession while reducing the impact in the measurement of the non perfect knowledge of the Earth's gravitational field:

$$\begin{cases} \dot{\Omega}_2^{L1}\boxed{\delta\bar{C}_{2,0}} + \dot{\Omega}_4^{L1}\boxed{\delta\bar{C}_{4,0}} + \dot{\Omega}_6^{L1}\boxed{\delta\bar{C}_{6,0}} + \boxed{\dot{\Omega}_{LT}^{L1}\mu} + \cdots = \boxed{\delta\dot{\Omega}_{res}^{L1}} \\ \dot{\Omega}_2^{L2}\delta\bar{C}_{2,0} + \dot{\Omega}_4^{L2}\delta\bar{C}_{4,0} + \dot{\Omega}_6^{L2}\delta\bar{C}_{6,0} + \dot{\Omega}_{LT}^{L2}\mu + \cdots = \delta\dot{\Omega}_{res}^{L2} \\ \dot{\Omega}_2^{LR}\delta\bar{C}_{2,0} + \dot{\Omega}_4^{LR}\delta\bar{C}_{4,0} + \dot{\Omega}_6^{LR}\delta\bar{C}_{6,0} + \dot{\Omega}_{LT}^{LR}\mu + \cdots = \delta\dot{\Omega}_{res}^{LR} \end{cases}$$

μ = 1 if General Relativity is correct
μ = 0 if Newtonian physiscs is correct

$$\dot{\Omega}^{comb} = \delta\dot{\Omega}_{res}^{L1} + k_1\delta\dot{\Omega}_{res}^{L2} + k_2\delta\dot{\Omega}_{res}^{LR}$$

- LT effect observable
- k_1 and k_2 are such that to cancel the unmodelled effects/errors of two even zonal harmonics (order *m*=0) of the Earth's gravitational field

$$\langle\dot{\Omega}_{class}\rangle_{sec} = -\frac{3}{2}n\left(\frac{R_\oplus}{a}\right)^2 \frac{\cos i}{(1-e^2)^2}\{-\sqrt{5}\bar{C}_{20}\} + \cdots$$

Model for the Earth’s gravitational field

In our analysis we taken into account the time dependency of the main even zonal harmonics on the basis of GRACE monthly solutions and not simply the constant values for these harmonics provided by their static solutions

C_{20}

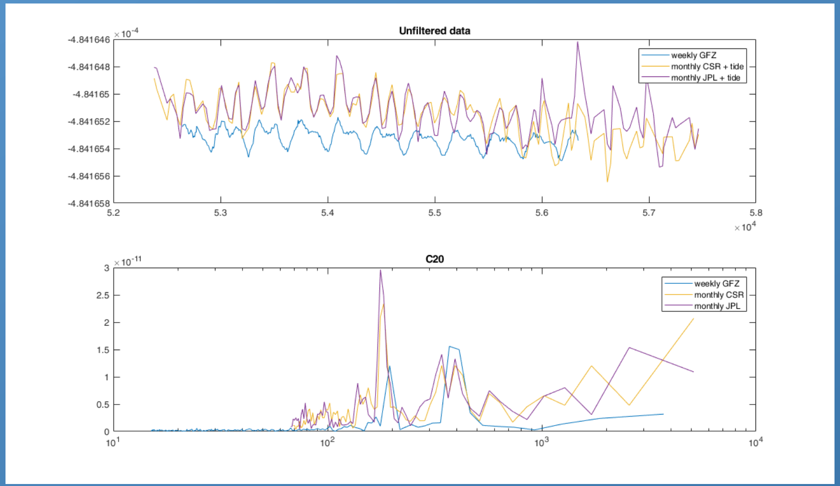

C_{40}

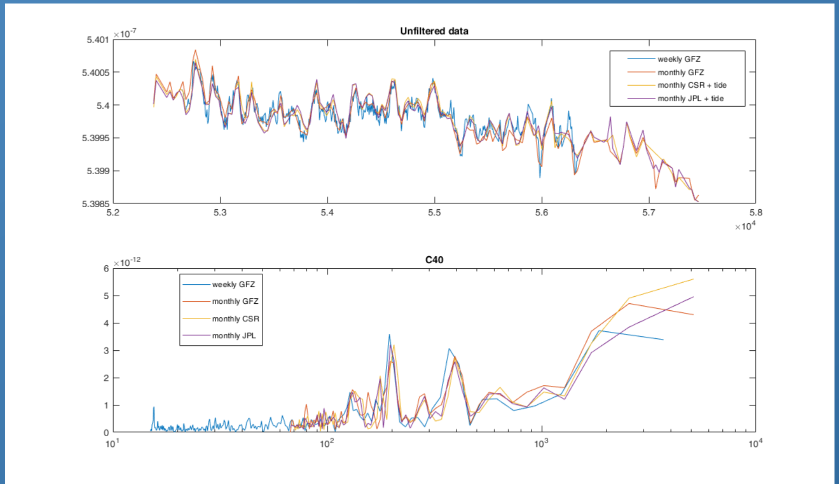

C_{60}

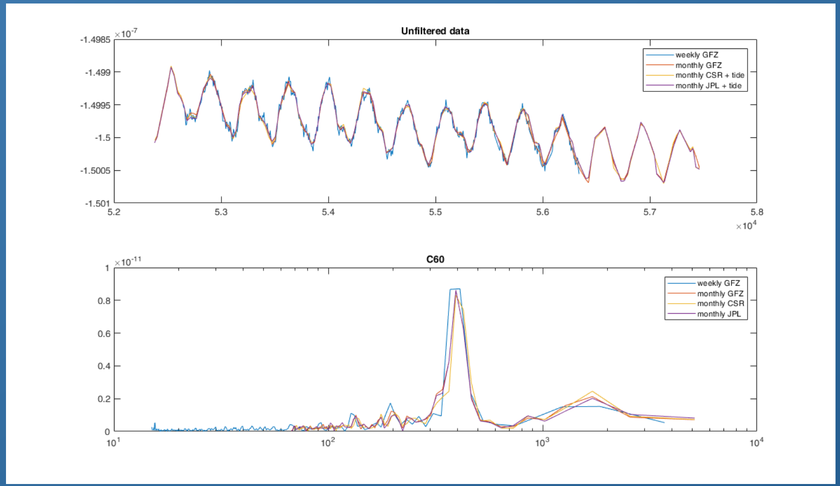

We fitted the first 15 even zonal harmonics from GRACE data with a linear trend, and we modelled them in our code as:

$$\bar{C}_{\ell,0}(t) = \bar{C}_{\ell,0}(t_0) + \dot{\bar{C}}_{\ell,0}(t - t_0)$$

Model for the Earth's gravitational field

We estimate the even zonal harmonics of low degree with the LT effect: comparison with GRACE results

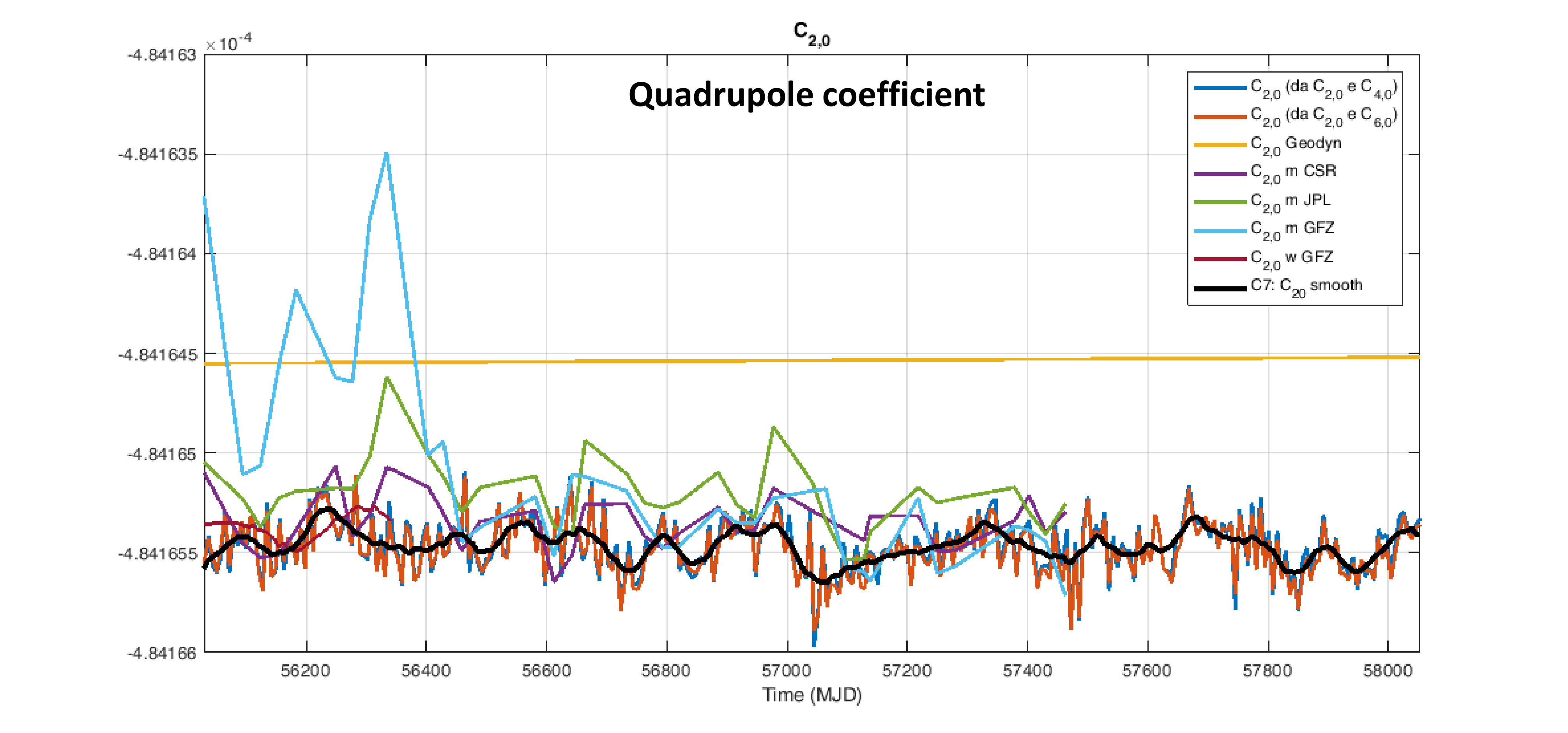

Model for the Earth's gravitational field

We estimate the even zonal harmonics of low degree with the LT effect: comparison with GRACE results

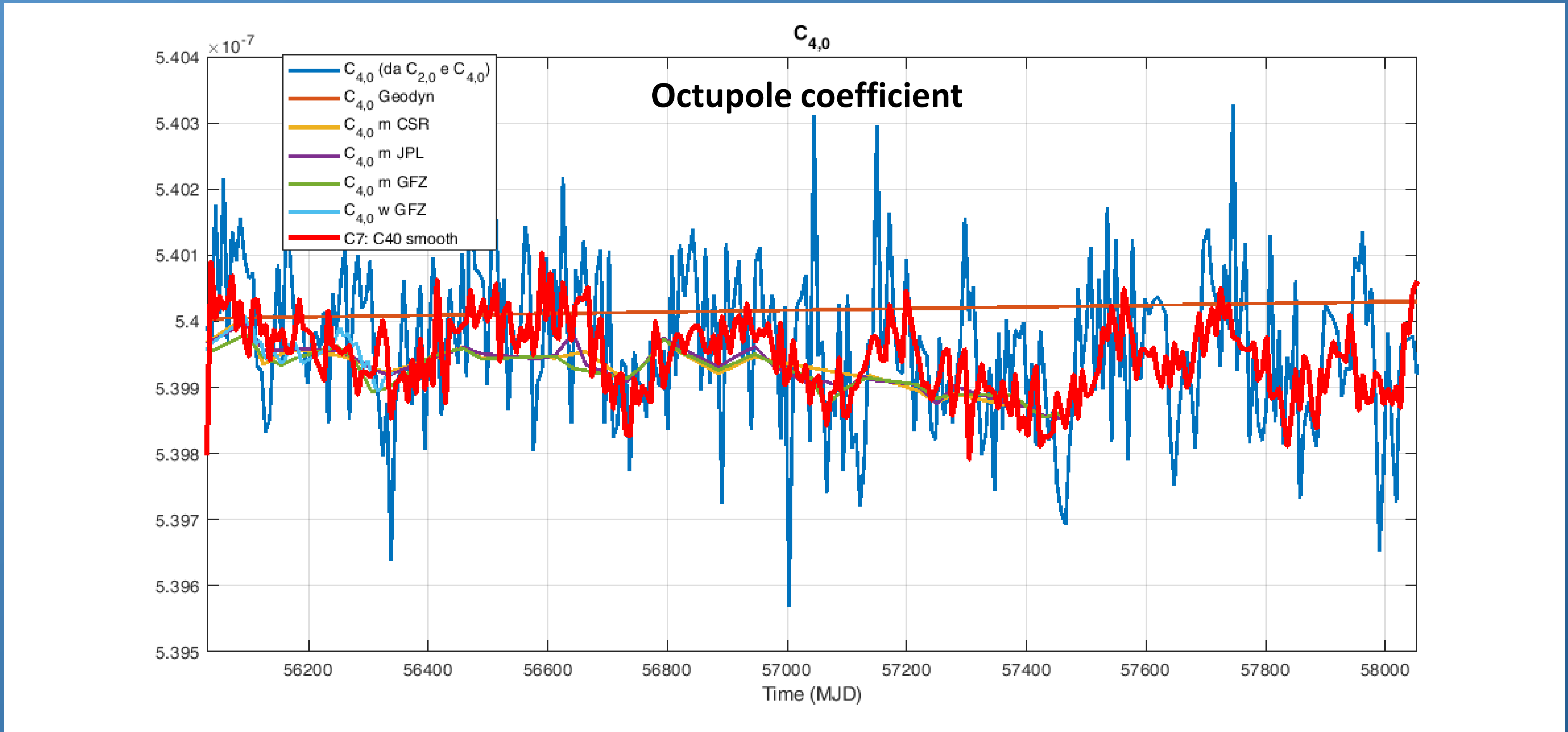

Model for the Earth's gravitational field

In our analysis we considered several solutions for the gravitational field of the Earth's from GRACE and GOCE missions:

1. EIGEN-GRACE02S (2004)
2. GGM05S (2014) (official field of the ILRS)
3. ITU_GRACE16 (2016)
4. Tonji-Grace02s (2017)
5. Tonji-Grace02k (2018)
6. GOSG01S (2018)

This allows us to better estimate and constrain systematics errors among the different solutions

TABLE III. The first five even zonal harmonics, and their rate, at the epoch J2000.0. These numerical values are valid and consistent values for the coefficients and their rates on the time span of about 6.5 years of our analysis, that starts from April 6, 2012.

Coefficient	Value	Rate $[yr^{-1}]$
2,0	$-4.8416528046720 \times 10^{-4}$	$\simeq 0.0$
4,0	$+5.4021417522157 \times 10^{-7}$	$-2.0790978790439 \times 10^{-11}$
6,0	$-1.4992584301767 \times 10^{-7}$	$-6.4611528233550 \times 10^{-12}$
8,0	$+4.9478882967800 \times 10^{-8}$	$\simeq 0.0$
10,0	$+5.3316662523196 \times 10^{-8}$	$+3.8368765925296 \times 10^{-12}$

Precise orbit determination (POD)

Analysis with GEODYN II over a time span of about 25.3 years (from October 30, 1992)

Geopotential (static part)	JGM–3; EGM–96; CHAMP; GRACE; GOCE
Geopotential (tides)	Ray GOT99.2
Lunisolar + Planetary Perturbations	JPL ephemerides DE–403
General relativistic corrections	PPN
Direct solar radiation pressure	Cannonball model
Albedo radiation pressure	Knocke–Rubincam model
Yarkovsk –Schach effect	Afonso et al., 1980, Farinella, 1996, LARASE (2018)
Earth–Yarkovsky effect	Rubincam 1987 – 1990 model
Spin–axis evolution	Farinella et al., 1996 model, LARASE (2018) model
Stations position	ITRF2000; ITRF 2008; **ITRF2014**
Ocean loading	Scherneck model (with GOT99.2 tides)
Polar motion	IERS (estimated)
Earth rotation	VLBI + GPS

Precise orbit determination (POD)

Range residuals of the three satellites (MJD=48925 - MJD=58165)

Analysis 0001 with empirical accelerations
Analysis 0002 with no empirical accelerations

with empirical accelerations

[cm]	Mean	Sigma
LAGEOS	-0.60	5.9
LAGEOS II	-0.75	3.5
LARES	-0.02	4.1

POD on a 25.3 yr timespan

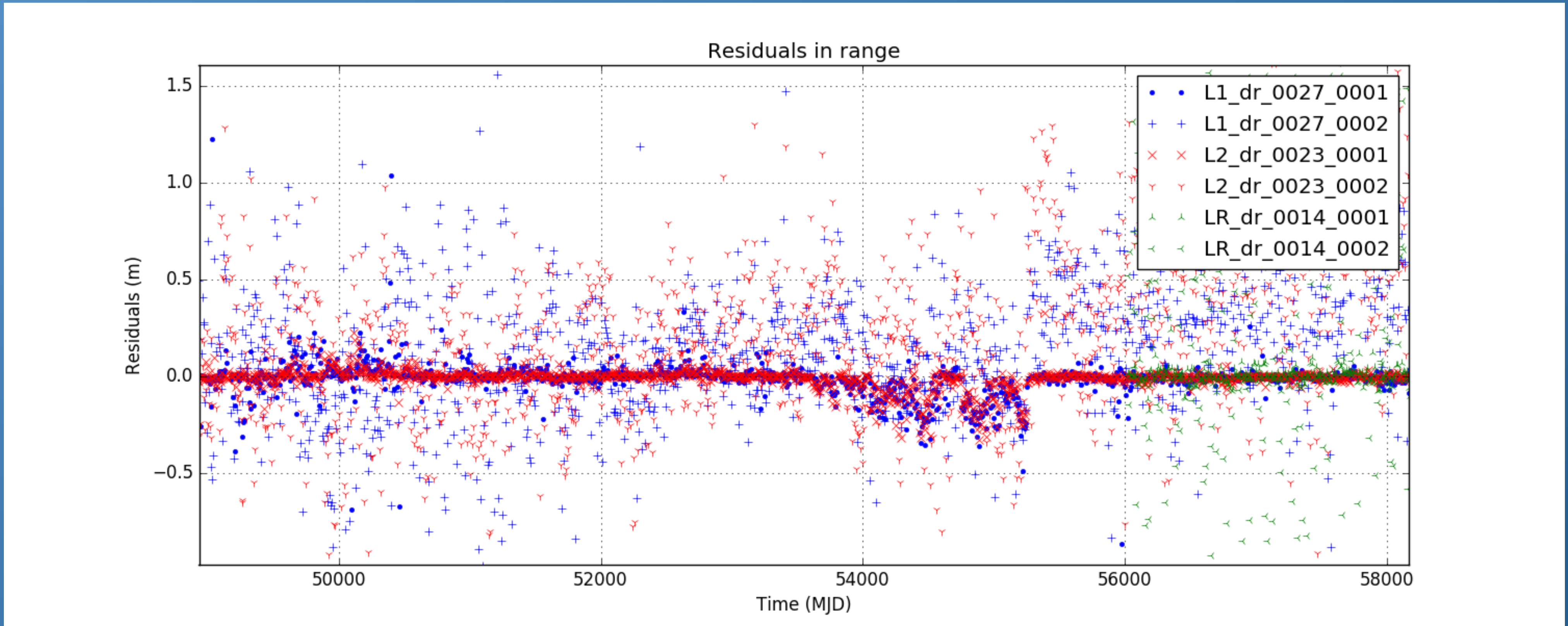

Precise orbit determination (POD)

RMS of the three satellites (MJD=48925 - MJD=58165)

Analysis 0001 with empirical accelerations
Analysis 0002 with no empirical accelerations

with empirical accelerations

[cm]	Mean	Sigma
LAGEOS	2.3	1.5
LAGEOS II	1.5	0.4
LARES	3.3	0.6

POD on a 25.3 yr timespan

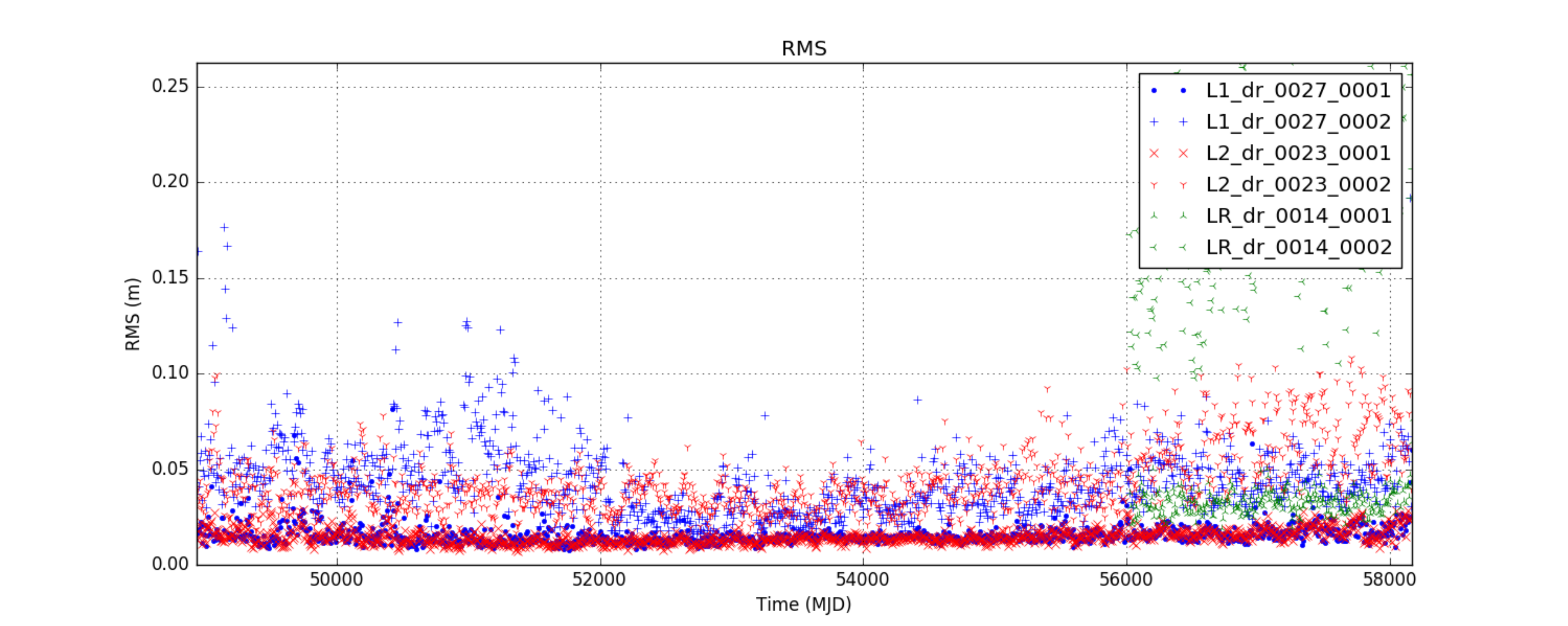

A new measurement of the Lense-Thirring effect

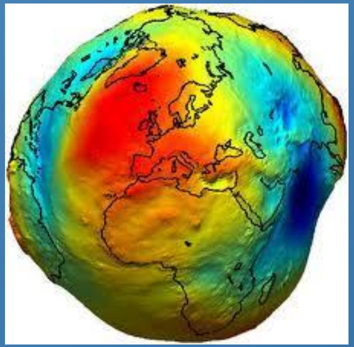

New aspects with respect to previous measurement of the LT effect:

- We considered several models for the background gravitational field of the Earth
  - This allows to highlight possible systematics among the different models
- For the first 10 even zonal harmonics we considered their explicit time dependency following the monthly solutions from GRACE measurements
  - This has reduced the systematic error of the background gravitational field
- Together with the relativistic LT precession we estimated also some of the low-degree even zonal harmonics (ℓ=even and m=0) of the background gravitational field
  - This allows to estimate the direct correlation between the relativistic LT precession with the coefficients of the gravitational field

A new measurement of the Lense-Thirring effect

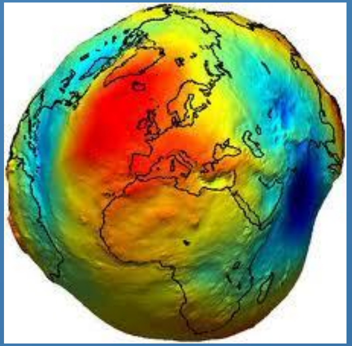

New aspects with respect to previous measurement of the LT effect:

- The relativistic LT precession has been measured both in the i) residuals of the rates of the combined nodes and in their ii) integration
  - This is the first time that the measurement has been performed on the rate of the combined observables: case i)
- The measurement has been obtained both via linear fits and non-linear fits
  - This is also the first time that a reliable measurement of the LT precession has been obtained by means of a simple linear fit

A new measurement of the Lense-Thirring effect

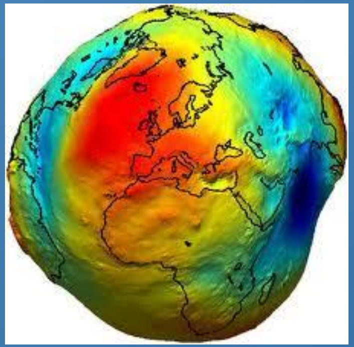

A new preliminary measurement of the LT effect

- We run GEODYN II over a time span of about 6.5 years (2359 days) from MJD 56023, i.e. April 6th 2012, and we computed the effects on the orbit elements of LAGEOS, LAGESOS II and LARES:
  - Background gravity model: GGM05S + other fields from GRACE and GOCE
  - Arc length of 7 days
  - No empirical accelerations
  - Thermal effects (Yarkovsky Schach and Rubincam) not modelled
  - General relativity modelled with the exception of the Lense-Thirring effect

TABLE I
RATE [MAS/YR] FOR THE LENSE-THIRRING PRECESSION ON THE RIGHT ASCENSION OF THE ASCENDING NODE OF LAGEOS, LAGEOS II AND LARES.

Orbital element	LAGEOS	LAGEOS II	LARES
$\dot{\Omega}^{LT}$	30.67	31.50	118.48

30 mas ≅ 1.8 m

$$\dot{\Omega}^{comb} = \delta\dot{\Omega}^{L1}_{res} + k_1 \delta\dot{\Omega}^{L2}_{res} + k_2 \delta\dot{\Omega}^{LR}_{res}$$

- LT effect observable
- k_1 and k_2 are such that to cancel the unmodelled effects/errors of two even zonal harmonics (order *m*=0) of the Earth's gravitational field: $C_{2,0}$ and $C_{4,0}$

$$V(r,\varphi,\lambda) = -\frac{GM_\oplus}{r}\left[1 + \sum_{\ell=2}^{\infty}\sum_{m=0}^{\ell}\left(\frac{R_\oplus}{r}\right)^{\ell} P_{\ell m}(\sin\varphi)\left(C_{\ell m}\cos m\lambda + S_{\ell m}\sin m\lambda\right)\right]$$

$$\dot{\Omega}_{class} = -\frac{3}{2} n \left(\frac{R_\oplus}{a}\right)^2 \frac{\cos i}{(1-e^2)^2} J_2 + \cdots$$

A new measurement of the Lense-Thirring effect

Residuals in the right ascension of the ascending node rate of the satellites

These residuals are due to unmodeled:

- periodic effects
  - thermal thrust effects
  - asymmetric reflectivity
  - tides + gravitational field
- secular effect related with the Lense-Thirring precession

Thermal effects[a]	LAGEOS	LAGEOS II	LARES
$\dot{\Omega}$	1052	570	211
$2\dot{\Omega}$	526	285	105
$\dot{\lambda}$	365	365	365
$2\dot{\lambda}$	183	183	183
$2(\dot{\Omega} - \dot{\lambda})$	280	111	67
$\dot{\Omega} + \dot{\lambda}$	271	953	497
Solid tides	LAGEOS	LAGEOS II	LARES
165.565	911	622	217
Ocean tides	LAGEOS	LAGEOS II	LARES
163.555	221	138	98

[a] Some of these spectral lines are also common to solid and ocean tides.

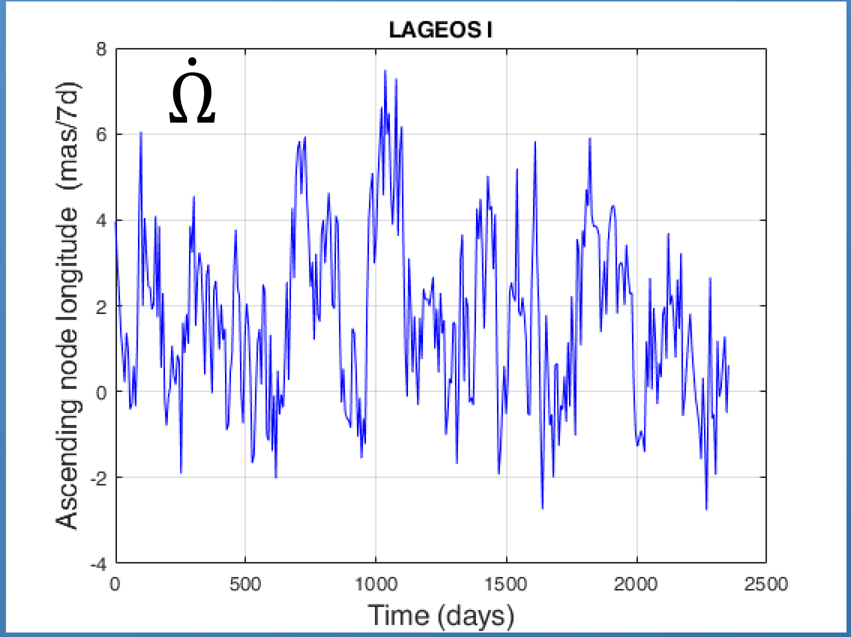

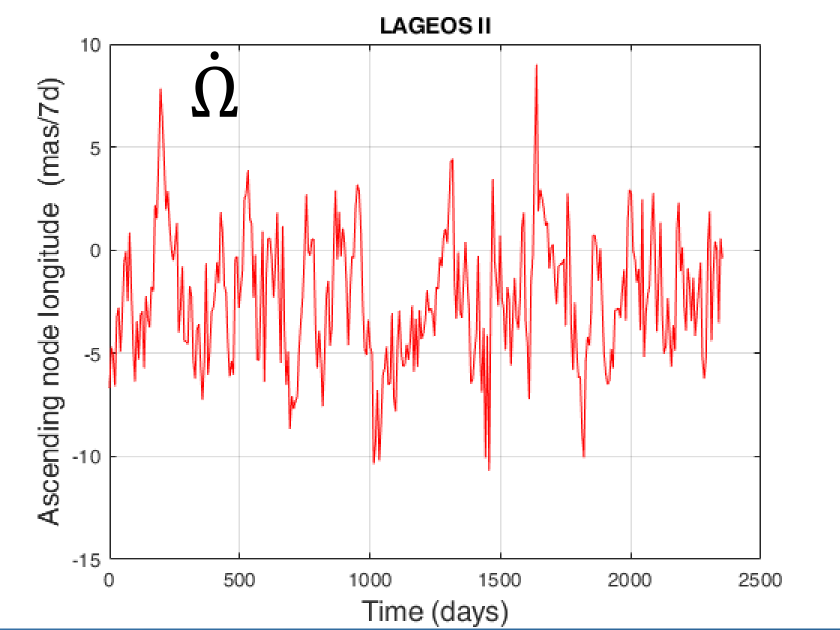

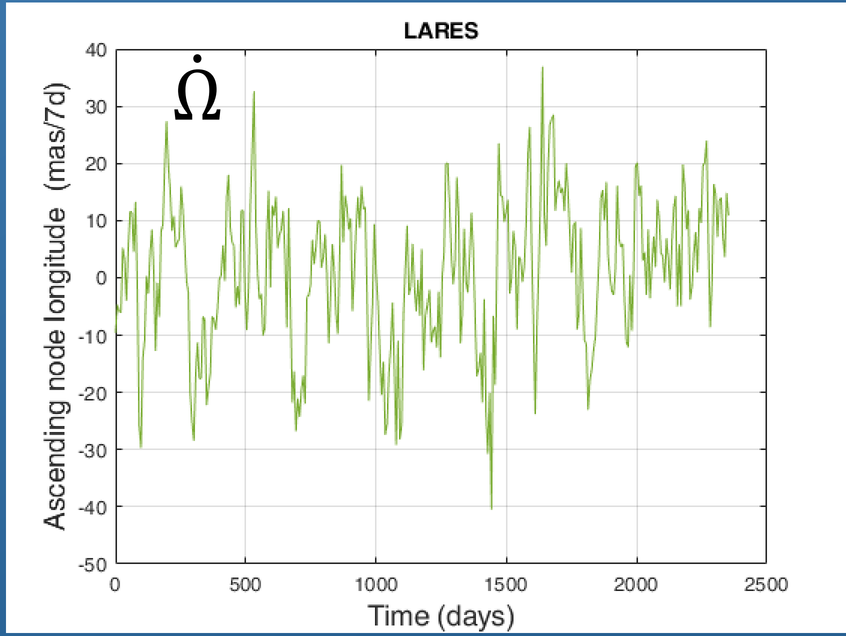

A new measurement of the Lense-Thirring effect

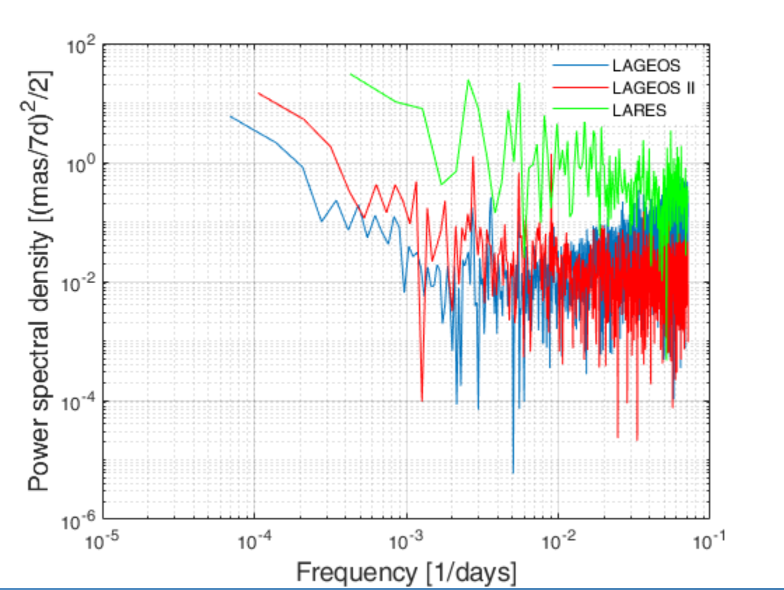

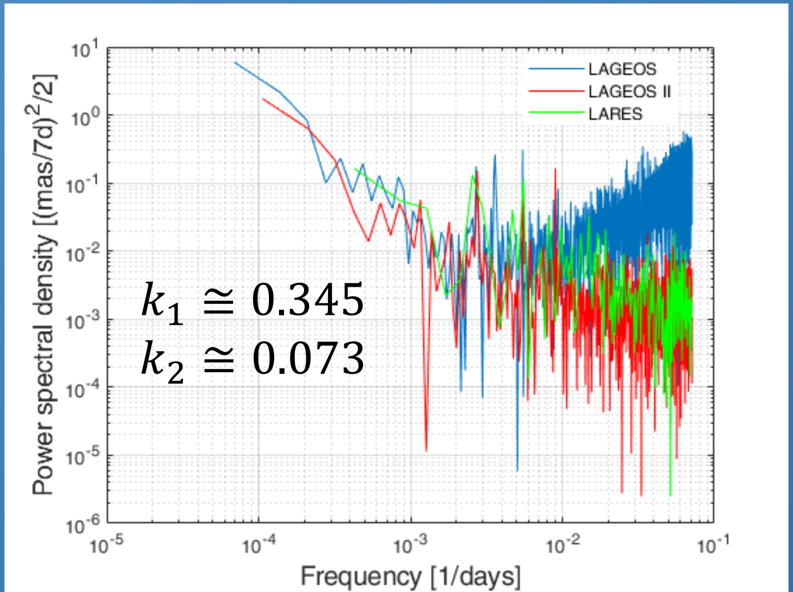

Spectral analysis of the R.A. of the ascending node rate of the satellites and of their combination:

$$\dot{\Omega}^{comb} = \delta\dot{\Omega}^{L1}_{res} + k_1\delta\dot{\Omega}^{L2}_{res} + k_2\delta\dot{\Omega}^{LR}_{res}$$

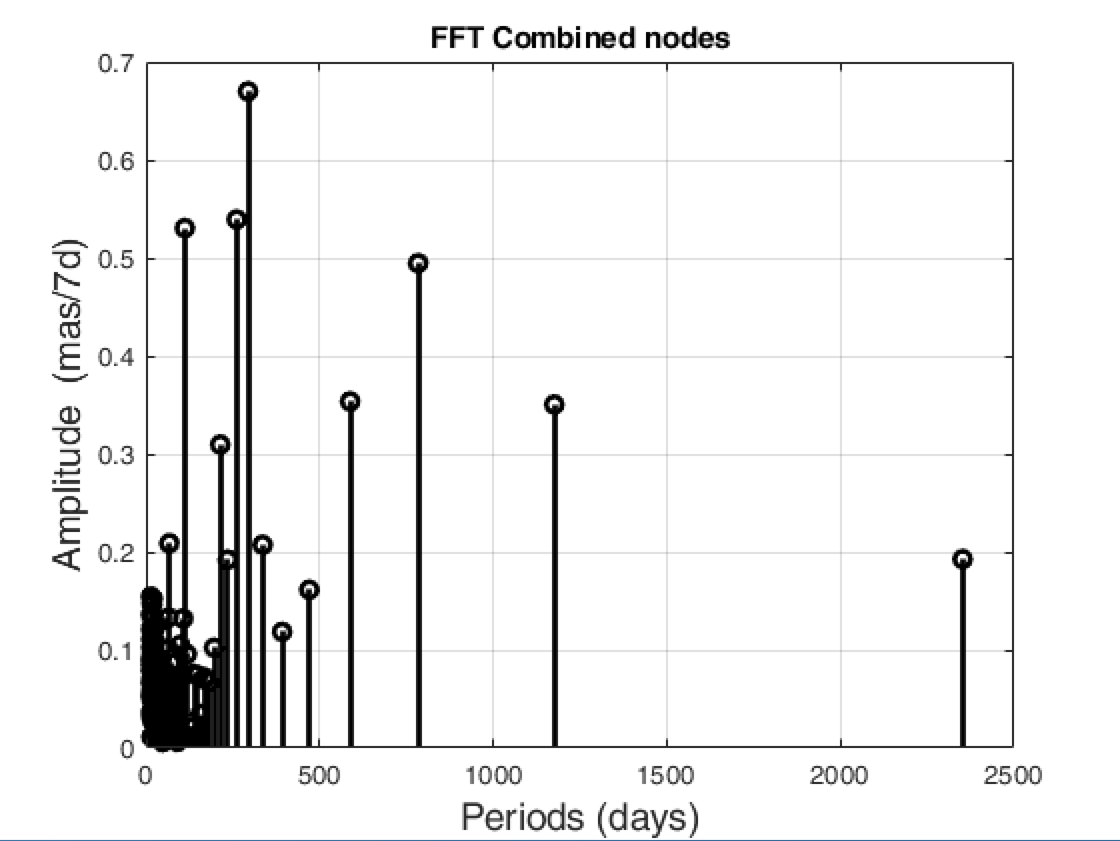

A new measurement of the Lense-Thirring effect

Combined residuals in the right ascension of the ascending node rate of the satellites and the of the combined nodes

$$\dot{\Omega}^{comb} = \delta\dot{\Omega}^{L1}_{res} + k_1\delta\dot{\Omega}^{L2}_{res} + k_2\delta\dot{\Omega}^{LR}_{res}$$

$$\dot{\Omega}^{comb}_{GR} = 50.17\ mas/yr$$

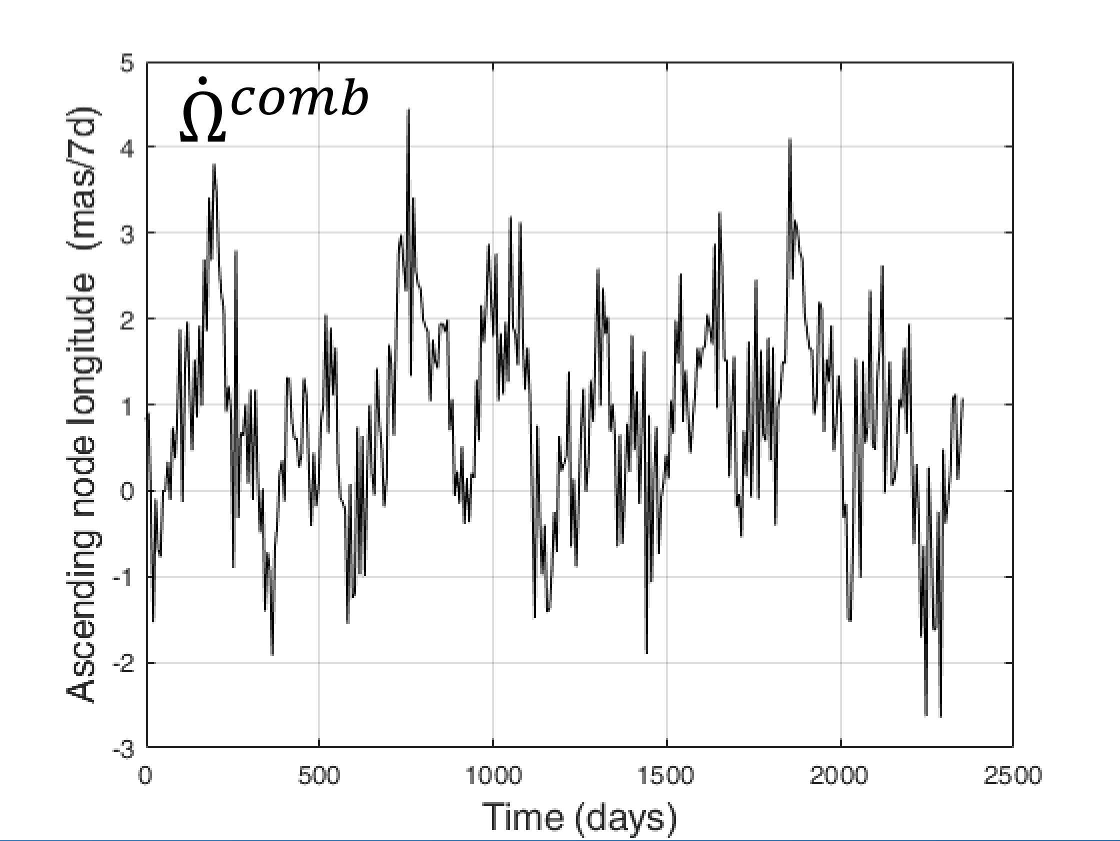

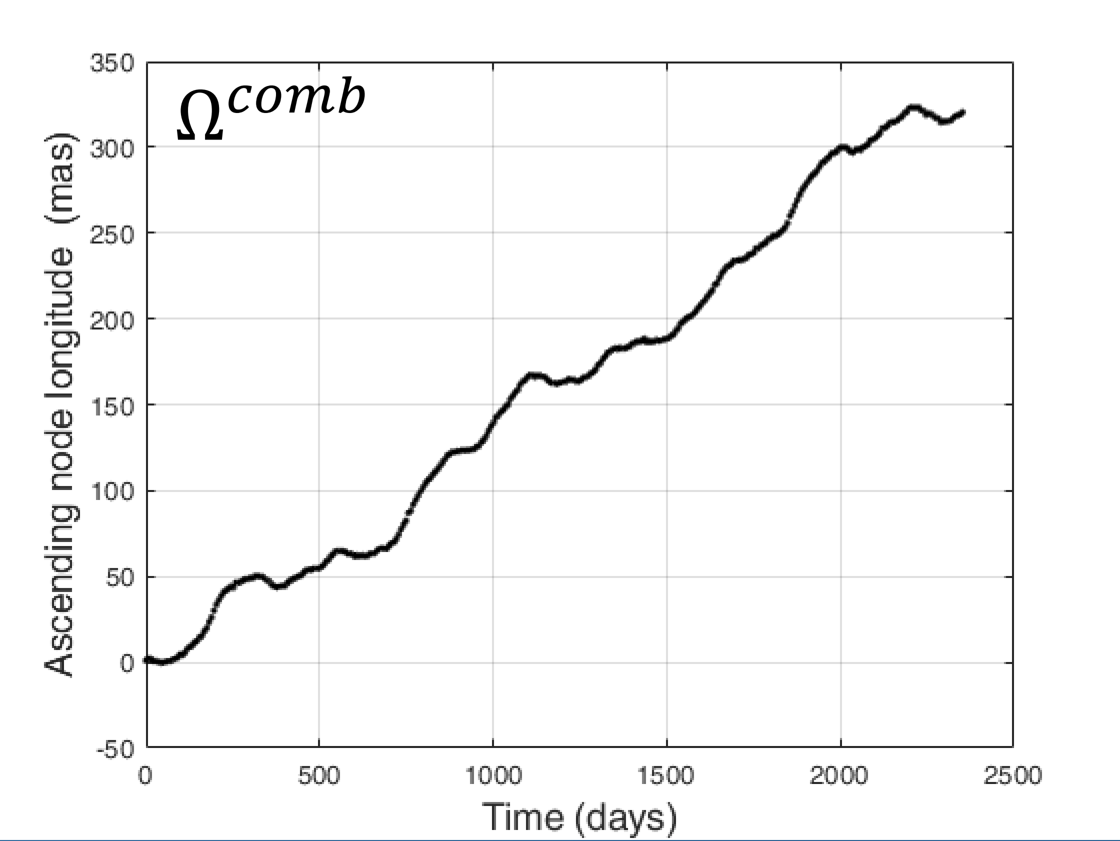

A new measurement of the Lense-Thirring effect

Correlations between the estimated quantities:

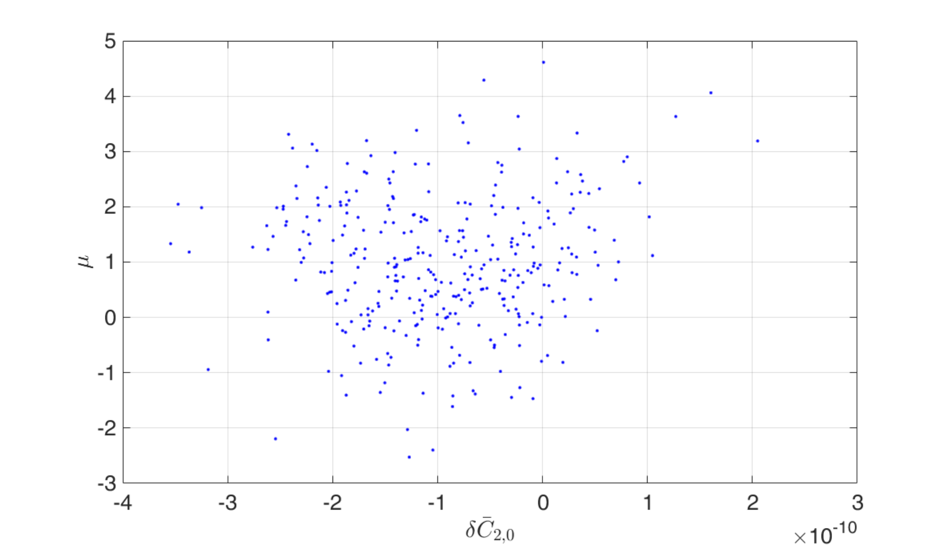

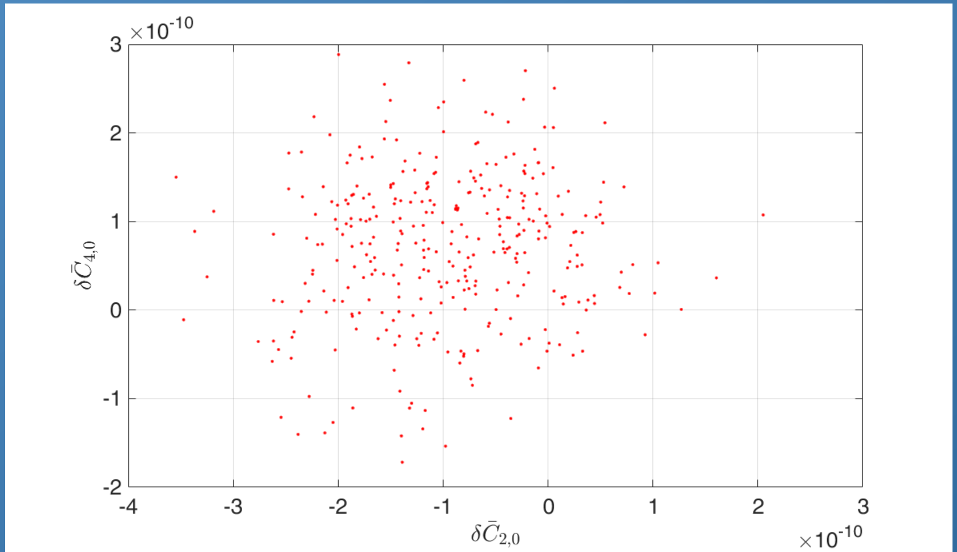

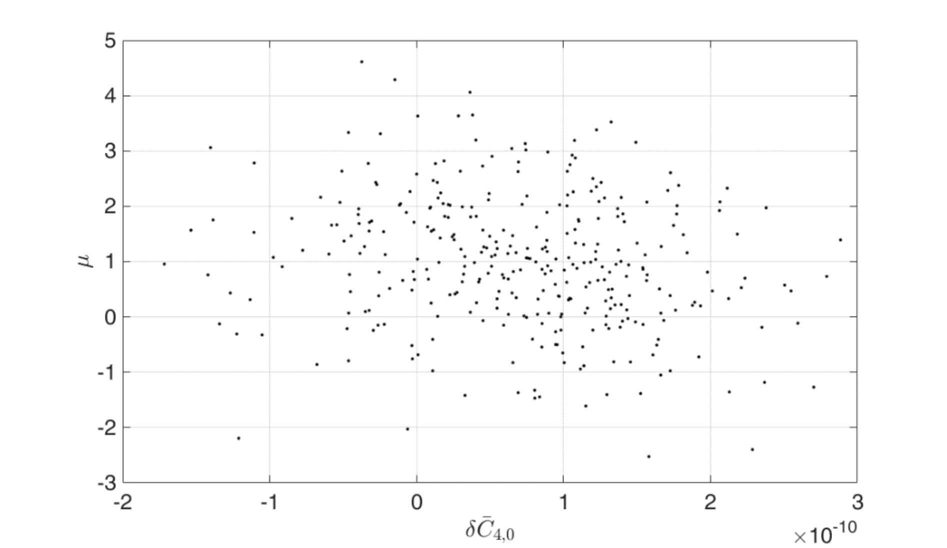

	$\delta C_{2,0}$	$\delta C_{4,0}$	μ
$\delta C_{2,0}$	**1.000**	**0.082**	**0.071**
$\delta C_{4,0}$	**0.082**	**1.000**	**–0.179**
μ	**0.071**	**–0.179**	**1.000**

A new measurement of the Lense-Thirring effect

Combined residuals in the right ascension of the ascending node rate of the satellites

$$\dot{\Omega}^{comb} = \delta\dot{\Omega}^{L1}_{res} + k_1\delta\dot{\Omega}^{L2}_{res} + k_2\delta\dot{\Omega}^{LR}_{res}$$

$$\dot{\Omega}^{comb}_{GR} = 50.17\ mas/yr$$

	Non-integrated residuals		Integrated residuals	
Model	Mean [mas/yr]	%	Slope [mas/yr]	%
GGM05S	49.61	−1.12	50.44 ± 0.37	+0.54 (0.74)
EIGEN-GRACE02S	49.05	−2.23	50.19 ± 0.37	+0.04 (0.74)
ITU_GRACE16	49.02	−2.29	50.14 ± 0.37	−0.06 (0.74)
Tonji-Grace02s	49.10	−2.13	50.25 ± 0.37	+0.16 (0.74)
Tonji-Grace02k	49.10	−2.13	50.25 ± 0.37	+0.16 (0.74)
GOSG01S	50.51	+0.68	51.62 ± 0.37	+2.89 (2.89)

$$\mu = \frac{\dot{\Omega}^{comb}}{\dot{\Omega}^{comb}_{GR}} = \begin{cases} 1 & \text{• In General Relativity} \\ 0 & \text{• In Newtonian physics} \end{cases}$$

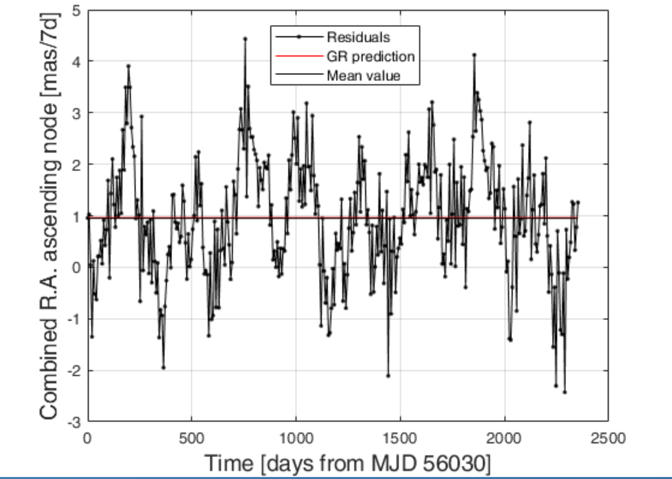

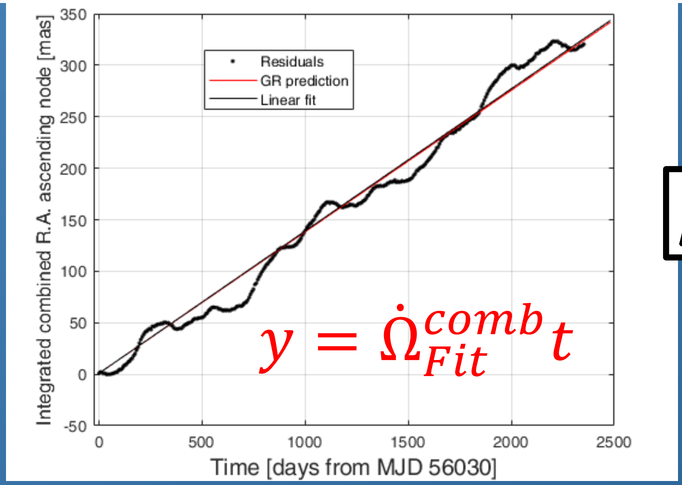

From the mean value:

$$\boldsymbol{\mu_{Fit} - 1 = -19 \times 10^{-3} \pm \delta\mu \pm \delta\mu_{sys}}$$

From the slope:

$$\boldsymbol{\mu_{Fit} - 1 = 2 \times 10^{-3} \pm 7 \times 10^{-3} \pm \delta\mu_{sys}}$$

A new measurement of the Lense-Thirring effect

A very preliminary estimate of the systematics

	δμ [%]	δμ [%]
Perturbations	**non.-int res.**	**int. res.**
Gravitational field	**2.20**	**0.74**
Periodic effects	**3.00 (7.00)**	**0.29 (0.54)**
de Sitter	**0.30**	**0.30**
RSS	**3.73 (7.34)**	**0.85 (0.96)**

$$\dot{\Omega}^{comb} = \delta\dot{\Omega}_{res}^{L1} + k_1\delta\dot{\Omega}_{res}^{L2} + k_2\delta\dot{\Omega}_{res}^{LR}$$

$$\dot{\Omega}_{GR}^{comb} = 50.17\ mas/yr$$

From the mean value:

$$\boldsymbol{\mu_{Fit} - 1 = -19 \times 10^{-3} \pm \delta\mu \pm 70\times10^{-3}}$$

From the slope:

$$\boldsymbol{\mu_{Fit} - 1 = 2 \times 10^{-3} \pm 7 \times 10^{-3} \pm 10\times10^{-3}}$$

Conclusions and future work

The activities of LARASE proceeds in terms of:

- development of new reliable models
  - ✓ for the (subtle) non-gravitational perturbations (Spin and Thermal Thrust effects)
  - ✓ as well as (in part) for the gravitational ones
- precise orbit determination (POD)
  - ✓ tracking data, models, stations, reference frames, …
- precise and accurate measurements of the gravitational interaction in the weak-field and slow-motion limit of General Relativity
  - ✓ Lense-Thirring and other effects …

Conclusions and future work

- in the centennial of the Lense-Thirring effect, we presented a new precise measurement for this relativistic precession on the combined orbits of the LAGEOS, LAGEOS II and LARES satellites: $\sim$ 0.2 %

- next goal is to provide a careful evaluation of the systematic errors of the measurement: $\sim$ 1-2 % (work in progress)

- the Lense-Thirring effect represents a weak manifestation of Mach's Principle and it proves that mass-currents in general relativity contribute to the curvature of space-time

Istituto Nazionale di Fisica Nucleare

LARASE is funded by the Italian INFN CSN2 on astroparticle physics

LASERRANGEDSATELLITESEXPERIMENT

LARASE website

http://larase.roma2.infn.it

IOP Publishing Classical and Quantum Gravity

Class. Quantum Grav. 32 (2015) 155012 (50pp) doi:10.1088/0264-9381/32/15/155012

Testing the gravitational interaction in the field of the Earth via satellite laser ranging and the Laser Ranged Satellites Experiment (LARASE)

D M Lucchesi[1,2,3], L Anselmo[2], M Bassan[3,4], C Pardini[2], R Peron[1,3], G Pucacco[3,4] and M Visco[1,3]

[1] Istituto di Astrofisica e Planetologia Spaziali (IAPS/INAF), Via del Fosso del Cavaliere 100, I-00133 Roma, Italy
[2] Istituto di Scienza e Tecnologie della Informazione (ISTI/CNR), Via G. Moruzzi 1, I-56124 Pisa, Italy
[3] Istituto Nazionale di Fisica Nucleare (INFN), Sezione di Roma Tor Vergata, Via della Ricerca Scientifica 1, I-00133 Roma, Italy
[4] Dipartimento di Fisica, Università di Roma Tor Vergata, Via della Ricerca Scientifica 1, I-00133 Roma, Italy

E-mail: david.lucchesi@iaps.inaf.it

Received 24 March 2015, revised 1 June 2015
Accepted for publication 15 June 2015
Published 14 July 2015

CrossMark

Many thanks for your kind attention

The LARASE collaboration

- IAPS/INAF, Roma: D. M. Lucchesi, C. Magnafico, R. Peron, M. Visco
- ISTI/CNR, Pisa: L. Anselmo, C. Pardini
- Dep. Physics, Tor Vergata-Roma: M. Bassan, G. Pucacco

Neutral drag perturbation for LARES

Comparison SATRAP - GEODYN

Decay of the semimajor axis of LARES on a timespan of 5.8 and the solar activity

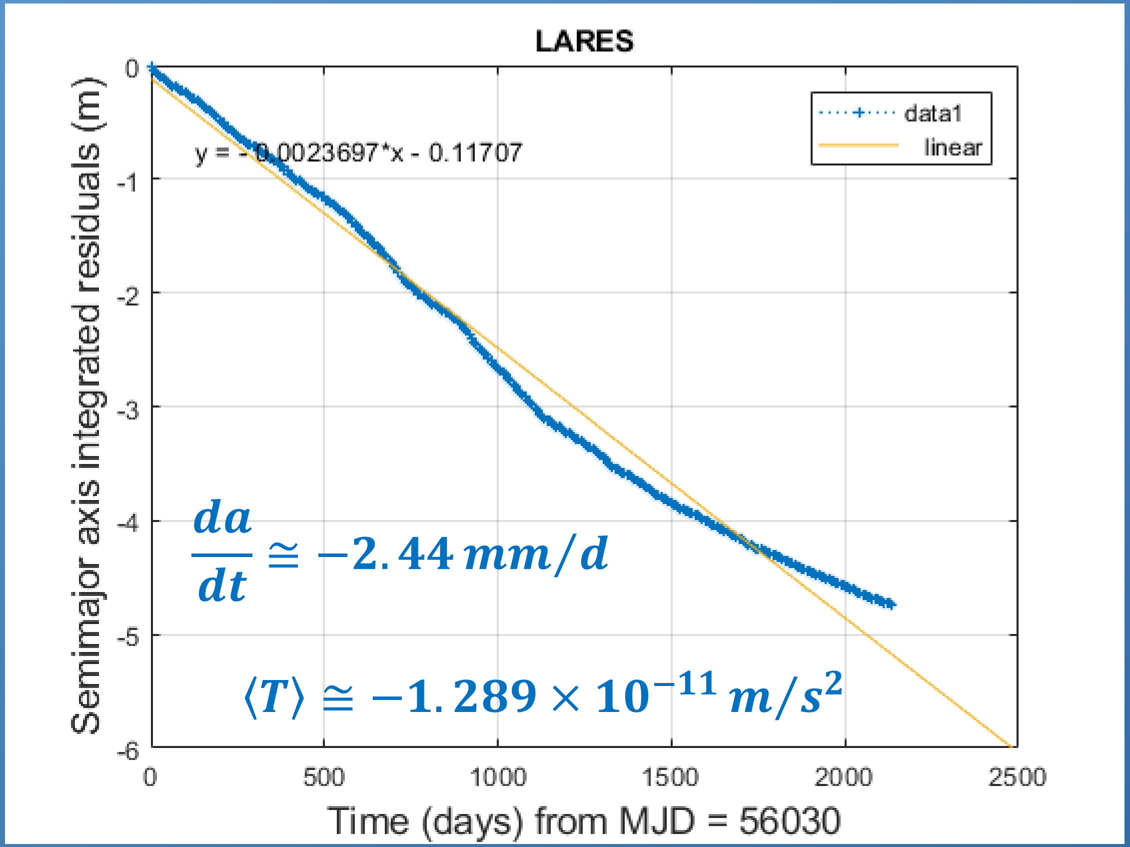

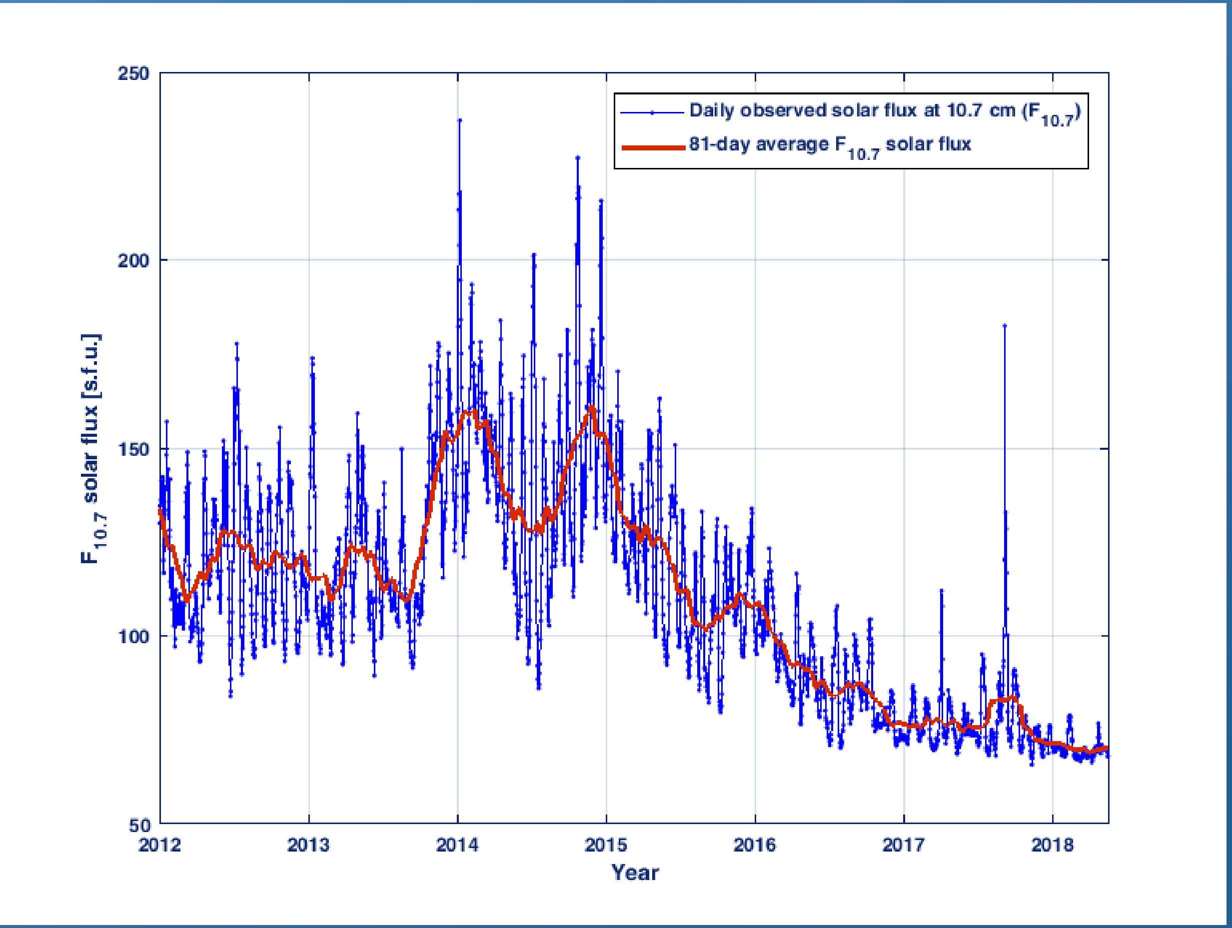

Comparison SATRAP - GEODYN

Gauss accelerations for LARES obtained by SATRAP

$$\frac{da}{dt} = \frac{2}{n\sqrt{1-e^2}}[T + e(T\cos f + R\sin f)] \qquad \frac{de}{dt} = \frac{\sqrt{1-e^2}}{na}[R\sin f + T(\cos f + \cos u)]$$

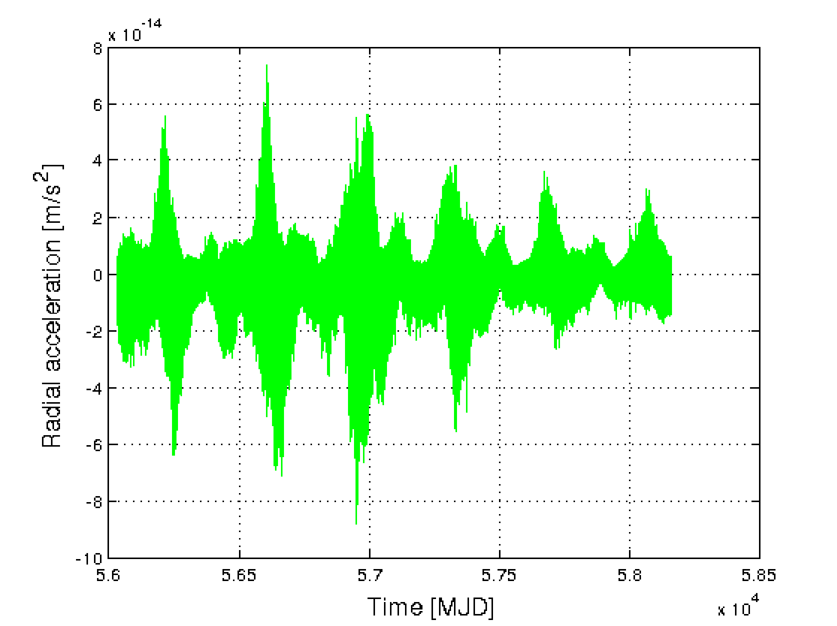

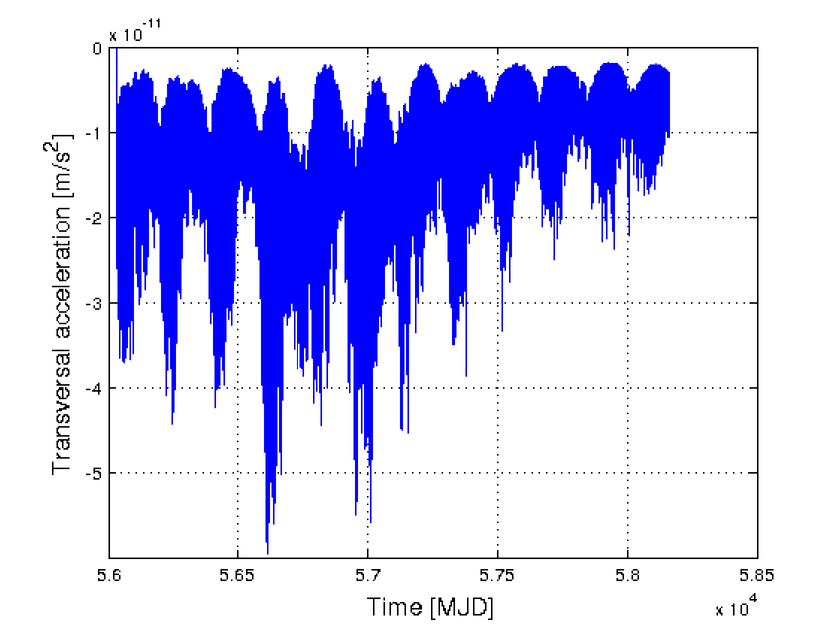

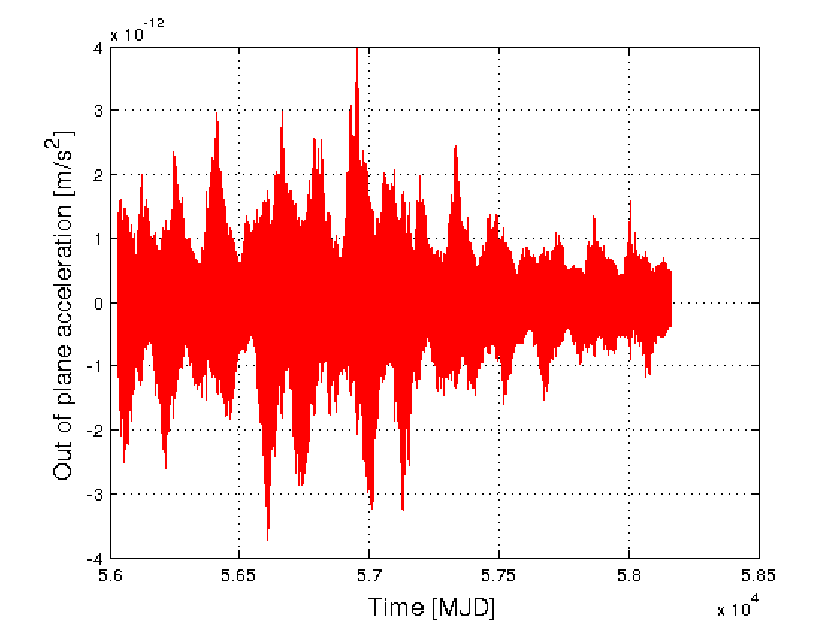

Comparison SATRAP - GEODYN

GEODYN residuals for the semi-major axis and eccentricity of LARES compared with their predictions for the neutral drag perturbation obtained with SATRAP and the application of Gauss equations

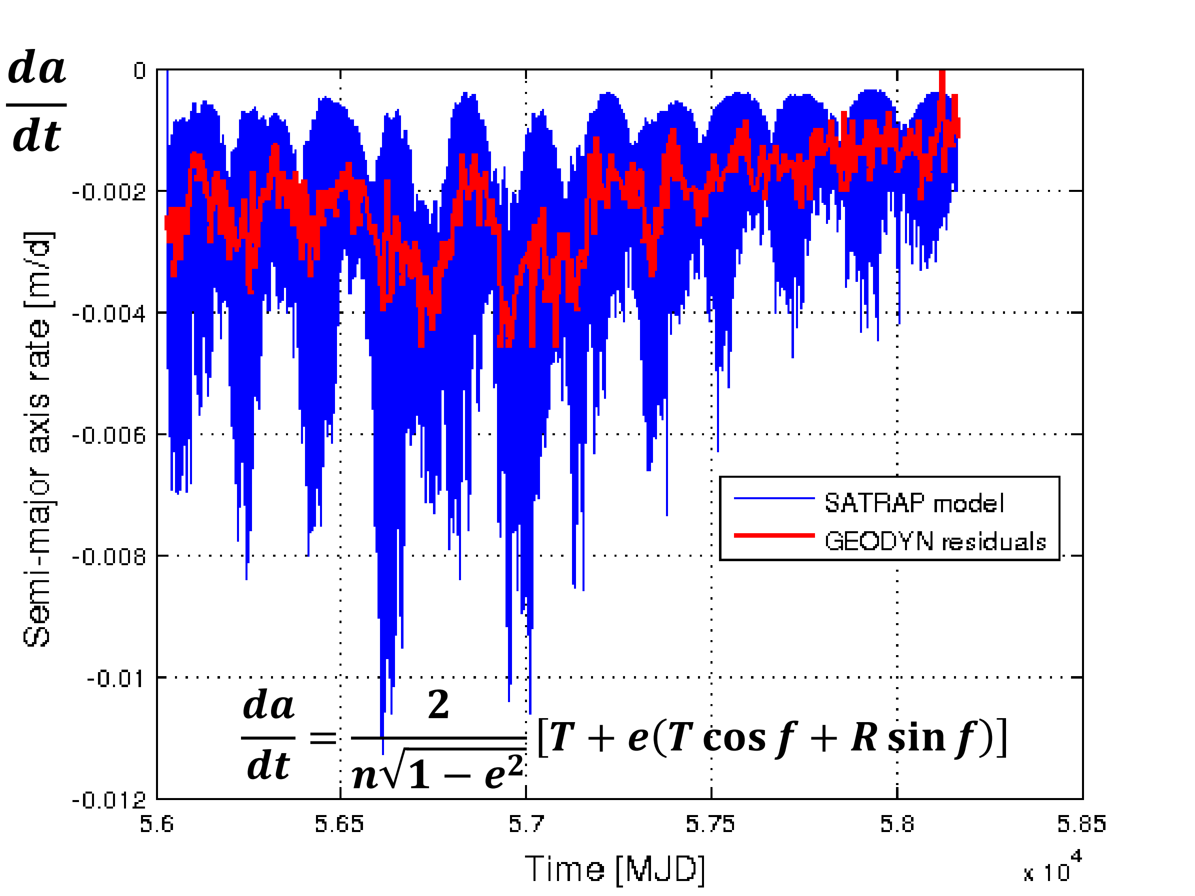

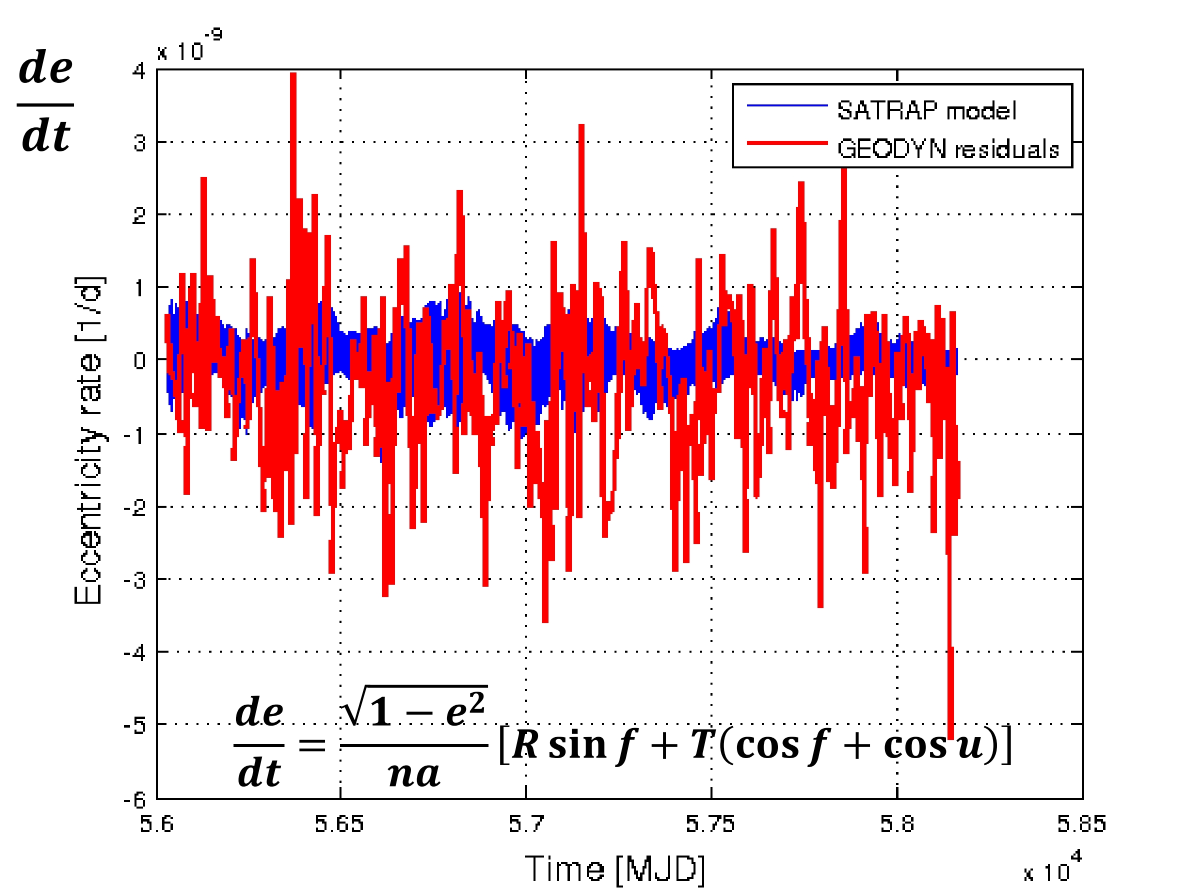

Constraints on 1/r^2

Yukawa-like long range interaction

Post data reduction analysis: 13-yr analysis of the LAGEOS II orbit (FIT)

Fit to the pericenter residuals:

$$\Delta\omega^{FIT} = a + b\cdot t + c\left(t - t_0\right)^2 + \sum_{i=1}^{n} D_i \sin\left(\frac{2\cdot\pi}{P_i}\cdot t + \Phi_i\right)$$

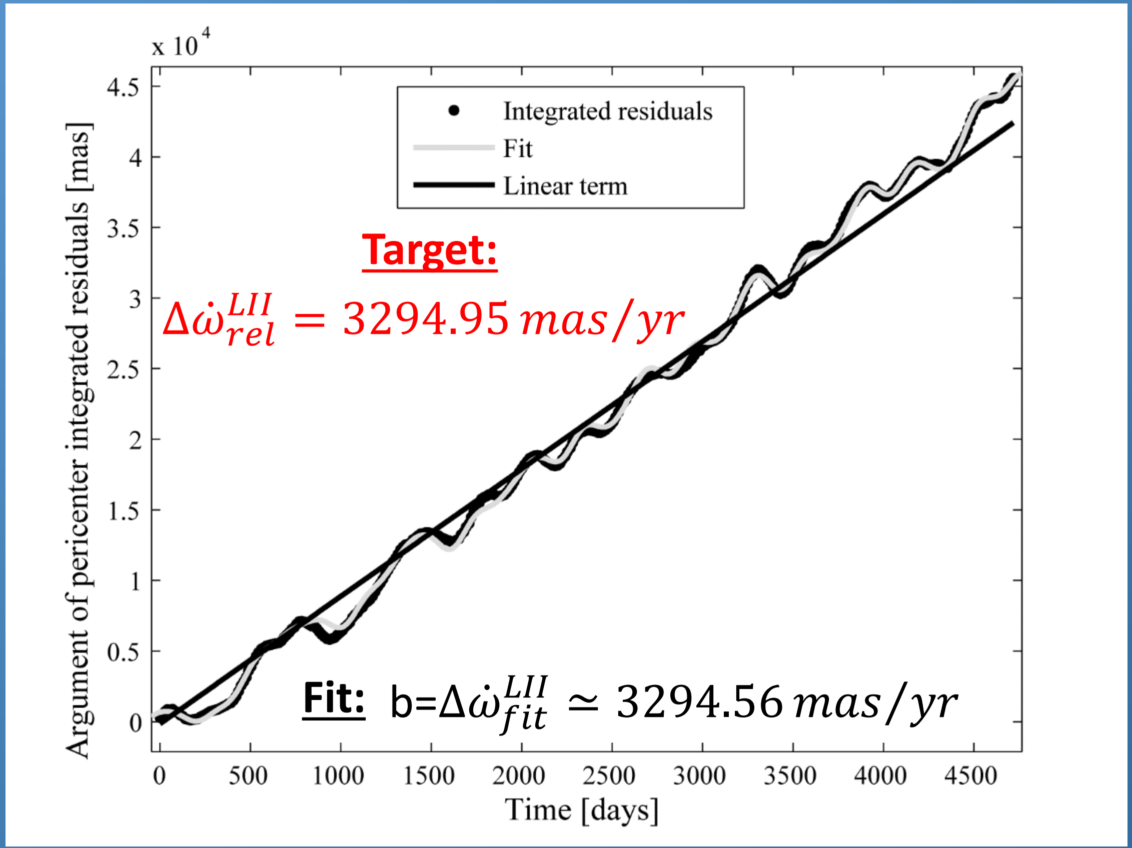

We obtained b ≅ 3294.6 mas/yr, very close to the prediction of **GR**.

The discrepancy is just **0.01%**.

From a sensitivity analysis, with constraints on some of the parameters that enter into the least squares fit, we obtained an upper bound of **0.2%**.

$$\Delta\dot{\omega} = \Delta\dot{\omega}_{GP} + \Delta\dot{\omega}_{NGP} + \varepsilon\cdot\Delta\dot{\omega}_{GR}$$

$$\varepsilon = 1 - (0.12 \pm 2.10)\cdot 10^{-3} \pm 2.5\cdot 10^{-2}$$

Yukawa-like long range interaction

The measurement of the pericenter advance

Why measuring the shift of the argument of pericenter?

- These very weak **NLRI** are usually described by means of a **Yukawa–like** potential with strength α and range λ:

$$V_{yuk} = -\alpha \frac{G_\infty M_1}{r} e^{-r/\lambda}$$

$$\alpha = \frac{1}{G_\infty}\left(\frac{K_1}{M_1} \cdot \frac{K_2}{M_2}\right)$$

$$\lambda = \frac{\hbar}{\mu c}$$

M_1 = Mass of the primary source;

M_2 = Mass of the secondary source;

G_∞ = Newtonian gravitational constant;

r = Distance;

α = Strength of the interaction; K_1, K_2 = Coupling strengths;

λ = Range of the interaction; μ = Mass of the light-boson;

$\hbar$ = Reduced Planck constant; c = Speed of light

- This **Yukawa–like** parameterization seems general (at the lowest order interaction and non-relativistic limit):

  - **scalar field with the exchange of a spin–0 light boson;**
  - **tensor field with the exchange of a spin–2 light boson;**
  - **vector field with the exchange of a spin–1 light boson;**

Yukawa-like long range interaction

Summary of the constraints obtained

TABLE XVIII. Summary of the results obtained in the present work; together with the measurement error budget, the constraints on fundamental physics are listed and compared with the literature.

Parameter	Values and uncertainties (this study)	Uncertainties (literature)	Remarks
$\epsilon_\omega - 1$	$-1.2\times10^{-4}\pm2.10\times10^{-3}\pm2.54\times10^{-2}$	$\cdots$	Error budget of the perigee precession measurement in the field of the Earth
$\frac{\lvert 2+2\gamma-\beta\rvert}{3}-1$	$-1.2\times10^{-4}\pm2.10\times10^{-3}\pm2.54\times10^{-2}$	$\pm(1.0\times10^{-3})\pm(2\times10^{-2})$[a]	Constraint on the combination of PPN parameters
$\lvert\alpha\rvert$	$\lesssim\lvert0.5\pm8.0\pm101\rvert\times10^{-12}$	$\pm1\times10^{-8}$[b]	Constraint on a possible (Yukawa-like) NLRI
$\mathcal{C}_{\oplus\mathrm{LAGEOSII}}$	$\leq(0.003\ \mathrm{km})^4\pm(0.036\ \mathrm{km})^4\pm(0.092\ \mathrm{km})^4$	$\pm(0.16\ \mathrm{km})^4$[c]; $\pm(0.087\ \mathrm{km})^4$[d]	Constraint on a possible NSGT
$\lvert 2t_2+t_3\rvert$	$\lesssim3.5\times10^{-4}\pm6.2\times10^{-3}\pm7.49\times10^{-2}$	3×10^{-3}[e]	Constraint on torsion

[a]From the preliminary estimate of the systematic errors of [166] for the perihelion precession of Mercury.
[b]From [167] with Lunar-LAGEOS *GM* measurements.
[c]From [5] and based on a partial estimate for the systematic errors.
[d]From [7] and based on the analysis of the systematic errors only.
[e]From [168] with no estimate for the systematic errors.

Lucchesi, Peron, Phy. Rev. D, 89, 2014

Reference: Coy, Fischbach, Hellings, Standish, & Talmadge (2003)

Yukawa-like long range interaction

Constraints on a long-range force: Yukawa like interaction

$$|\alpha| \cong |(0.5 \pm 8) \cdot 10^{-12} \pm 101 \cdot 10^{-12}|$$

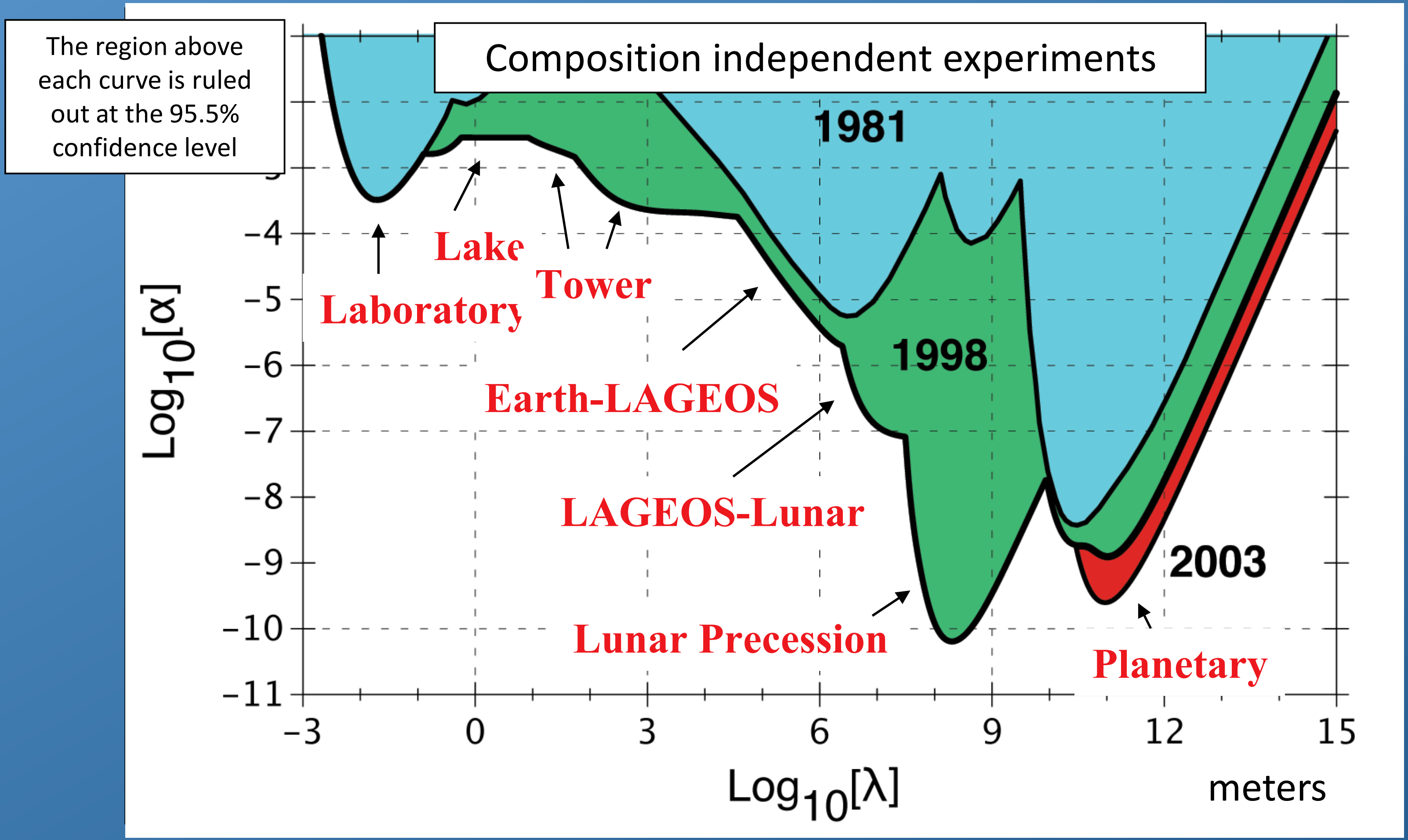

Previous limits with **LAGEOS's**:

$$|\alpha| < 10^{-5} \div 10^{-8}$$

Reference: Coy, Fischbach, Hellings, Standish, & Talmadge (2003)

Yukawa-like long range interaction

Constraints on a long-range force: Yukawa like interaction

$$|\alpha| \cong |(0.5 \pm 8) \cdot 10^{-12} \pm 101 \cdot 10^{-12}|$$

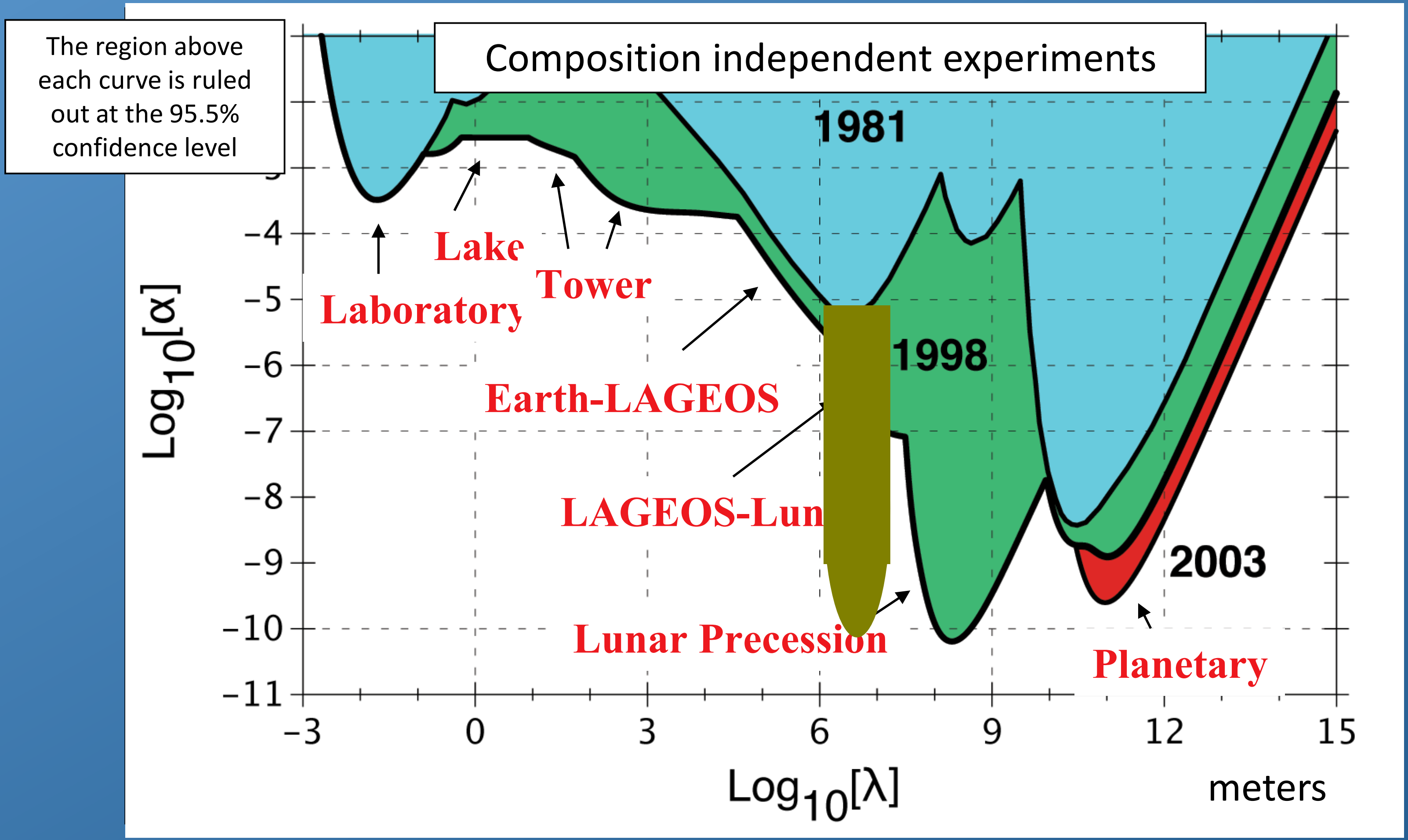

Previous limits with **LAGEOS's**:

$$|\alpha| < 10^{-5} \div 10^{-8}$$

Reference: Coy, Fischbach, Hellings, Standish, & Talmadge (2003)

Yukawa-like long range interaction

Constraints on a long-range force: Yukawa like interaction

$$|\alpha| \cong |(0.5 \pm 8) \cdot 10^{-12} \pm 101 \cdot 10^{-12}|$$

The region above each curve is ruled out at the 95.5% confidence level

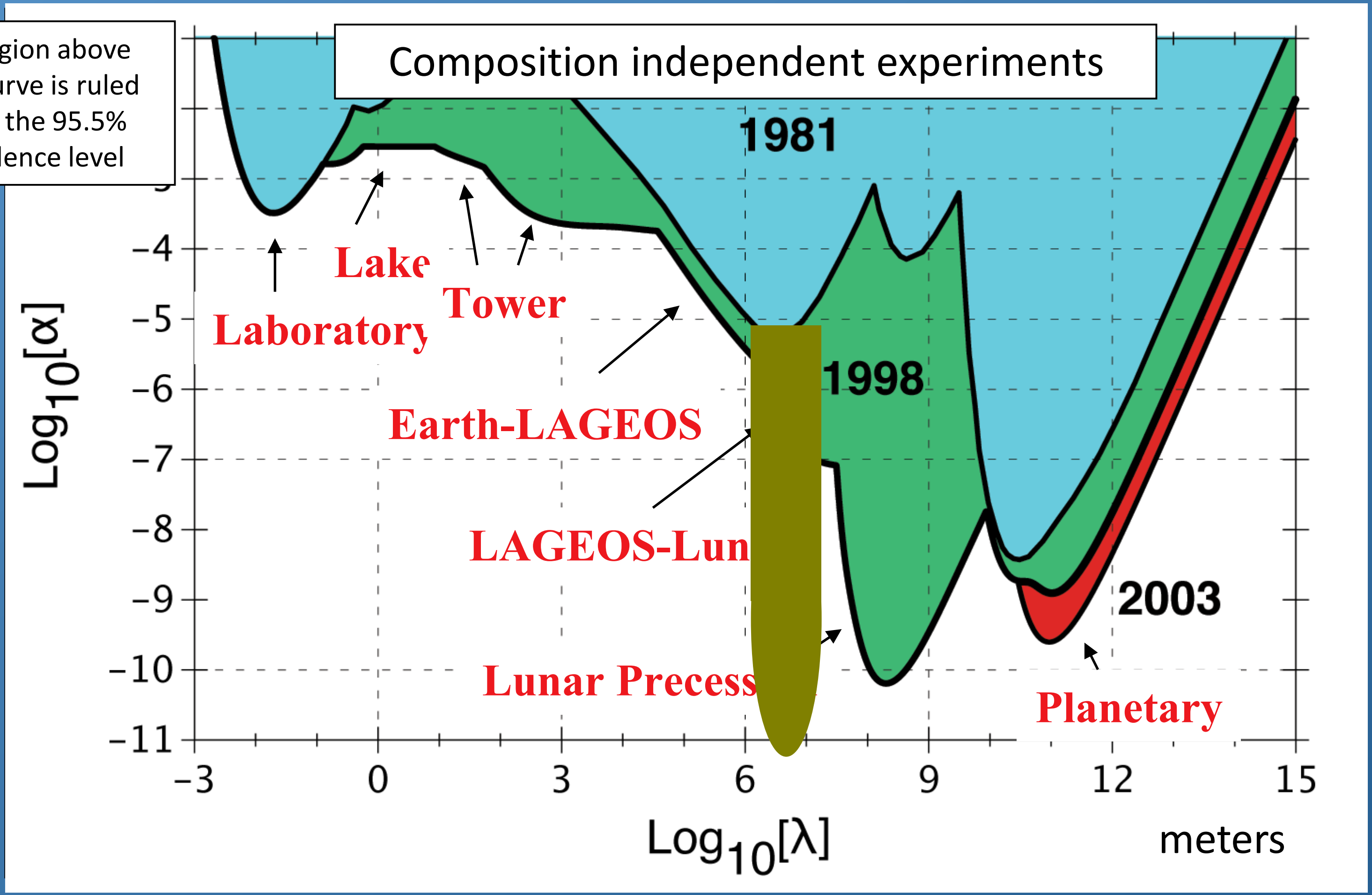

Previous limits with **LAGEOS's**:

$$|\alpha| < 10^{-5} \div 10^{-8}$$